[Supplementary material]

A new chronological model for the Bronze and Iron Age south Caucasus: radiocarbon results from Project ArAGATS, Armenia

Sturt W. Manning[1,*], Adam T. Smith[2], Lori Khatchadourian[3], Ruben Badalyan[4], Ian Lindsay[5], Alan Greene[6] & Maureen Marshall[7]

[1] *Department of Classics, 120 Goldwin Smith Hall, Cornell University, Ithaca NY 14853, USA*

[2] *Department of Anthropology, 261 McGraw Hall, Cornell University, Ithaca NY 14853, USA*

[3] *Department of Near Eastern Studies, 409 White Hall, Cornell University, Ithaca NY 14853, USA*

[4] *Institute of Archaeology and Ethnography, National Academy of Sciences, 15 Charents Street, Yerevan, 0025, RA, Armenia*

[5] *Department of Anthropology, Purdue University, 700 W. State Street, Suite 219, West Lafayette IN 47907, USA*

[6] *Institute for the Study of the Ancient World, New York University, 15 East 84th Street, New York, NY 10028, USA*

[7] *Russian, East European, and Eurasian Center, University of Illinois at Urbana-Champaign, 105 International Studies Building, Champaign IL 61820, USA*

[*] *Author for correspondence (Email: sm456@cornell.edu)*

Here we present a detailed discussion of the ArAGATS radiocarbon dates and their Bayesian chronological modelling. All Project ArAGATS survey and excavation data, including sample context descriptions, are publically available at: https://aragats.gorgesapps.us.

Radiocarbon dates

The radiocarbon dates on organic samples collected by Project ArAGATS and available for this paper comprised mainly wood charcoal. Except for those studied for dendrochronological/dendroarchaeological purposes, and before the Cornell Tree Ring Laboratory became involved with the ArAGATS work, the charcoal samples sent for radiocarbon dating were, unfortunately, not identified to species. A subsequent study of wood

charcoal from the collections offers a guide to the likely species (Jude et al. 2016). We discuss the topic of allowance for in-built age below. The other samples comprise some shorter-lived material (i.e. bone, teeth) or short-lived material with annual growth (i.e. barley, peas). Where available, discrete short-lived samples (and ideally sets thereof) from secure, primary contexts provide the best dating evidence. Securely associated short-lived samples, like annual seeds or similar materials, form the prime focus of modern high-resolution archaeological chronology via radiocarbon (e.g. Waterbolk 1971; Ashmore 1999; Bronk Ramsey *et al.* 2010; Bayliss *et al.* 2011; Boaretto 2015). They should offer ages contemporary with their context; that is, the 'dated event', the organic sample, is approximately the same age as the 'target event', the archaeological context. We note that we have not carried out detailed investigation on bone and teeth samples with respect to diet and any possible freshwater reservoir effect (e.g. Higham *et al*. 2010; Philippsen 2013). However, we see no evidence for any substantive offset to older radiocarbon ages for the bone or tooth samples, as would be expected if such a freshwater reservoir-effect applied. Indeed, the bone and tooth samples are often at the more recent end of the date ranges from the better defined contexts, following, or contemporary with, the most recent ages from the charcoal samples. This suggests they likely offer accurate ages. There is also very little evidence from the excavations for the exploitation of fish, and the local rivers are headwaters with little prospect of substantial fishing. Thus we do not consider a freshwater reservoir-effect as a substantive issue.

Most samples reported were dated at the University of Arizona AMS radiocarbon facility (https://ams.arizona.edu/), code AA. A few samples were AMS radiocarbon dated at the Klaus-Tschira laboratory in Mannheim (http://www.cez-archaeometrie.de/?page_id=718&lang=en), code MAMS. Additional samples were run at the former Heidelberg Radiocarbon Laboratory, code Hd. In our dating model, we consider comparisons for the Early Bronze 1 period at the ArAGATS site of Gegharot with two nearby sites, Aparan III and Karnut, where 4 radiocarbon dates were variously run at Arizona, Lyon and Berlin (these dates are listed in our OxCal runfile, see below). The samples received the pretreatment and processing that was routine given the normal procedures by each laboratory at the time (laboratory processes were not a research aspect of this project). The Project ArAGATS radiocarbon dates employed in this study are listed in Dataset S1 and the preferred OxCal model (Model 3) with these data is defined in Table S1.

Bayesian chronological modelling

Bayesian chronological modelling allows the integration of probabilities and constraints from a set(s) of radiocarbon dates (and their calendar dating probabilities, as determined via the radiocarbon calibration curve) with archaeological sequence information and other inputs, such as historical dates, or other prior information. This integration of knowledge (probabilities) allows us to achieve refined calendar dating probabilities for the samples and the archaeologically defined groupings of samples, and to quantify specified relationships and queries (Bronk Ramsey 1995; 2009a; Bayliss 2009). A focus on quality control and explicit reporting to enable subsequent testing and replication is key to robust work (Bayliss 2015), and we provide details of our model and approach as well as the full OxCal runfile below. The method has revolutionized archaeological chronology in many areas of the world and periods of (pre)history. In this first major study for the South Caucasus, we employ the OxCal 4.3 software (Bronk Ramsey 2009a; 2009b) and the mid-latitude Northern Hemisphere IntCal13 radiocarbon calibration dataset (Reimer *et al*. 2013) with the default calibration curve resolution of 5 years.

Our model—see Table S1—orders and groups the ArAGATS radiocarbon data from the initial Early Bronze Age to the modern period with a focus on (i) the Early Bronze Age, and (ii) the Late Bronze Age through Iron 3 period based on the long-term multidisciplinary archaeological investigations of Project ArAGATS (Smith *et al*. 2004; Badalyan *et al*. 2008; Smith *et al*. 2009; Badalyan *et al*. 2010; Badalyan *et al*. 2014; Khatchadourian 2014). The data are grouped and ordered on the basis of their archaeological associations and stratigraphic relations. The whole model structure and results from Model 3 are shown in Figure S1 A to J below. Here, we review and explain the key elements of our data and model.

(i) Radiocarbon dates on wood charcoal samples include in-built age (IA), unless they comprise bark or outermost tree rings or were part of the stated tree-ring-^{14}C-wiggle-match sequences (see below). The charcoal samples employed in the wiggle-matches have been identified to species (see Dataset S1). While other samples were not identified before they were dated, Jude et al.'s (2016) study of wood charcoal remains from Gegharot provides a reasonable view of the likely tree species involved. Importantly, none are extremely long-lived. Thus, we may assume that in most cases there is only a modest 'old wood' effect. We can consider this issue by running our dating model (Table S1) with all the non-wiggle-match charcoal as well as other shorter/short-lived samples considered with the OxCal General Outlier Model (Bronk

Ramsey 2009b): see Figures S2 A-E. We refer to this as Model 1. If we consider the probable outliers identified in Model 1 (those with Posterior values >5 versus the Prior value of 5: thus e.g. "O:11/5" in Figure S2), indicated in bold in Figures S2 A-E, we may observe:

(a) For the EBA all the 'outlier' charcoal samples are older (non-modelled versus modelled probability distributions); hence, as would be expected, a few charcoal samples are 'old wood'—whether inner rings from older trees, or residual/re-used wood. Two samples only appear to reflect substantially older wood (AA109433, AA102807). Date AA72067 on seeds is the other notable outlier—its age is rather more recent than expected from the other dates and it might suggest late EB activity, in the twenty seventh to twenty sixth centuries BC, after most of the rest of the evidence represented at Gegharot. At present, the significance of this single date—whether an outlier, or somehow intrusive, or in fact important evidence of late EB activity—is unclear.

(b) For the LB data we also observe that most of the dates on charcoal samples identified as outliers are cases where the non-modelled date is a little older than the modelled date range. Once again, these appear to represent a few cases of 'old wood', as would be expected, with just a handful of substantially older dates: AA66896, AA66892, AA72052, AA82786, AA66885). There are also, however, a few cases where dates on charcoal samples are more recent than expected. Apart from laboratory measurement error/noise, especially where these outliers also exhibit unsatisfactory OxCal agreement values (A values less than 60), these might indicate possible unrecognized later activity reaching into the early Iron Age (clearest examples are AA82787, AA92846). One reason for employing the Charcoal Plus Outlier model (see below) in our preferred Model 3 is to allow for these occasional later dates. Among the dates on short-lived samples, which are unfortunately very few, there are two minor possible outliers (Posterior v. Prior of 6>5 in each case). In each case, the measured dates are slightly more recent than the modelled ages. When we subsequently apply the Charcoal Plus Outlier model, and assume that the charcoal samples range typically from somewhat older than the context to dates for the context itself (as is clearly the case), then these dates are no longer outliers: see Model 3, shown in Figure S1.

(c) For the Iron Age data we again observe that a few of the measured ages on charcoal samples are, as expected, older than the modelled ages for the relevant context (AA86869, AA72372, AA92841, AA92842, AA96522, AA96523, AA72368). Only one sample is a conspicuous outlier and in the unexpected direction: AA40148, where the measured age is much

more recent than the modelled age. This date is placed on archaeological grounds and via associations in stratum 2c, Iron 1a. If it is not ascribed to laboratory error/noise, this date may indicate unrecognized later tenth to ninth century BC activity/use at Gegharot.

Based on the assessment from Model 1, and the general understanding of the in-built age issue in radiocarbon dates on sets of wood charcoal samples, we apply the Charcoal Plus Outlier model (Dee *et al*. 2013; Dee & Bronk Ramsey 2014) on all dates derived from charcoal, except those forming part of tree-ring wiggle-match sequences. We use the Charcoal Plus Outlier model because it is more realistic than the original Charcoal Outlier model (Bronk Ramsey 2009b), as explained in Dee *et al*. (2013); Dee & Bronk Ramsey (2014), and in particular because it allows for a few samples that post-date the expected context date range. Note: to use the Charcoal Plus Outlier model the user needs first to create a Prior file in OxCal with the data set listed in Table S3 below (compare with rounded data version in Dee *et al*. 2013: Table S6).

(ii) To test whether or not dates on shorter or short-lived samples are likely outliers and to downweight such data, we employ the General Outlier model in OxCal (Bronk Ramsey 2009b).

(iii) Where we have tree-ring sequenced sets of radiocarbon dates for so-called "wiggle-matching" of a dendroarchaeological sample (Bronk Ramsey *et al*. 2001; Galimberti *et al*. 2004), we employ the RScaled Outlier model from OxCal (Bronk Ramsey 2009b) on the basis that in such cases the error should be on the radiocarbon and not calendar time-scale.

(iv) To consider and highlight the significance of the choice and use of outlier models, we also ran the model without any outlier models applied. This is Model 2. In Table S2 we show the modelled calendar age ranges for various elements of the model from both Model 2 and the preferred Model 3, in which what we consider to be an appropriate outlier strategy was applied (and also the variations from Model 3a). Typically Model 3, with outlier strategy, removes some of the oldest probability from ranges, which seems appropriate given an assumption of in-built age for some/many charcoal samples, and reduces the extent of the overall modelled ranges a little.

(v) Beyond the formal outlier models, (i)-(iii) above, we can assess the individual elements in the model and the model overall via the diagnostic tools available in OxCal. Individual dates can be checked via their Agreement Index value (how successfully the modelled dating probability overlaps with the original non-modelled dating probability), which should be ≥60 per cent. In a large, complex model like this one, it is to be expected that at least some data will fall

below the 60 per cent threshold, with real concern directed towards values well below 60 per cent. Of greater importance are the overall model agreement indices. The Amodel value indicates whether the overall model agrees with the data. A value over *c.* 60 per cent indicates good agreement. The Aoverall value is a product of all the individual agreement indices and again should be over *c.* 60 per cent for a successful model. In initial runs of the dataset comprising the final dating model in Table S1 a very few dates were found to be unacceptable outliers (very large outliers or divergent values, which rendered it difficult to get the model to converge and run at all). These outliers have been excluded from the current models employed here (Models 1, 2, 3). Outliers amount to 6 dates, 2 of which were also excluded because their find contexts differed sharply from the resulting age determination, suggesting an unrecognized issue of residual or intrusive material. These samples are indicated by comments (//) in the runfile in Table S1. The model (Model 1 and Model 3) (see Table S1 for Model 3) runs with Amodel values typically (from several runs) around 68 per cent for Model 1 and between *c*. 80 and 91 for Model 3, and Aoverall values around 83 per cent for Model 1 and 75–76 for Model 3—all above the *c*. 60 per cent threshold. Model 2, applying the OxCal General Outlier model to all the charcoal dates in order to gauge the scale of the in-built age/old-wood offset that typically applies (see above) unsurprisingly has poor Amodel and Aoverall values (typical values: Amodel 13.9, Aoverall 14.9) since a number of dates are outliers, as shown in Figure S2 and discussed in (i) (a)-(c) above. In Model 3 only eight individual data have agreement indices below 60 per cent and only two are below 30 per cent: AA109429 and AA72067. However, AA109429 is not usually an outlier via the General Outlier model, where it has a value of only 5 v. 5 (Posterior v. Prior) (occasionally it is 6>5). Thus, we assume it is in fact acceptable. AA72067 is a minor possible outlier (8>5). On current evidence, it is impossible to say whether this seed sample is an outlier due to laboratory error/noise, or archaeological association, or instead evidence of activity/use in the area that is slightly later than the rest of its currently assigned phase. Considering the currently available Gegharot 1b dataset, the most efficient solution is a relatively constrained (shorter) overall phase: 27-102 years at 68.2 per cent probability and 8–168 years at 95.4 per cent probability in Model 3. Indeed, even if a (uniform probability) longer phase length of somewhere between 0-300 years is suggested, the model tends towards the shorter end, calculating 138–186 years at 68.2 per cent probability and 123–218 years at 95.4 per cent probability. The latest dates for the End of 1b Boundary only move from 2683 BC to 2647 BC at

95.4 per cent probability. Thus positive evidence for a longer 1b phase requires additional new data which supports the reality of the AA72067 date. Overall, of the samples tested versus the General Outlier model (n=25) in Model 3, only AA72067 is flagged as a possible outlier (relatively minor) with a Posterior v. Prior of 8>5. There are no remaining large or very obvious outliers in the model. In Figures S1 C-I, the individual Agreement Index values, A, are indicated for each individual radiocarbon date, as are the Outlier values (O). For the charcoal samples (and the Charcoal Plus Outlier model) these outlier values are all 100/100 and irrelevant in this regard. For the pre-model wiggle-match analyses, Figures S1A-B, only the Outlier values are shown.

(vi) The key evidence for the dating of the end of the Late Bronze Age at Gegharot (Ar/Ge) comes from a set of radiocarbon dates on samples of barley (*Hordeum vulgare* L.) from the end of the Late Bronze 2 occupation of the site. The find context is securely stratified and dates the close of LBA destruction, confirmed by the radiocarbon dates. There are 6 radiocarbon dates, four from Arizona and two from Mannheim. The model in its preparatory portion (before the ArAGATS sequence) considers both the weighted average of these data, and the modelling of the six date set with Tau_Boundary paired with a Boundary, to best estimate this destruction. Modelling the six dates as a group of events assumed to be distributed exponentially towards the end of the context, which is to say the end of LB2, with the exponential (Tau Boundary) approach is particularly useful because it assumes that all the radiocarbon-dated samples are older than the end of the context, most by very little but perhaps some even by a significant margin. This ensures that dates on individual residual samples or individual samples older for some other reason will not lead to an overestimation of the date for the end of the context. In each case, runs of the model found that AA104305C was a likely outlier, either as the clear 97 per cent probability outlier (whereas all the other five samples have outlier probabilities of less than 5 per cent) applying the SSimple Outlier model to the R_Combine of the set in OxCal when obtaining a weighted average value (Ward & Wilson 1978), or as the one possible minor outlier in the Phase (typically 6 per cent outlier probability v. Prior 5 per cent value) applying the General Outlier model for a Tau_Boundary paired with a Boundary analysis in OxCal (Bronk Ramsey 2009b). Thus, we exclude AA104305C from our final model. The limits of the 95.4% probability calendar range from the exponential model for the end of phase Boundary “Ar/Ge LB2 Destruction Tau_Boundary”, 1251 to 1093 BC, are employed as the limits for the dating of the end of the Ar/Ge Late Bronze 2 in the subsequent model.

(vii) Some of the wood-charcoal samples recovered had sufficient tree-rings to be suitable for dendrochronological examination. These have been dated using sets of tree-ring sequenced radiocarbon dates ("wiggle-matching") employing the defined sequence (D_Sequence) function in OxCal to best estimate the last extant tree-ring (Bronk Ramsey *et al*. 2001; Galimberti *et al*. 2004). In no case was bark or waney edge preserved, so the last extant tree-ring is merely a *terminus post quem* (TPQ) for the date the original trees were felled and this wood first used by humans. In a couple of cases for deciduous oak (*Quercus* sp.) samples, as part of this minimum TPQ estimate we also allowed for missing sapwood based on the minimum age of the original tree in approximate terms, since there are no data for typical sapwood counts for oaks from the Caucasus, in contrast for example to data available in Europe (Haneca *et al*. 2009). Numbers for samples, whether with "rings" or RY (Relative Years), are the specific set of tree-rings dated in each case. The wiggle-match age is treated as the mid-point of each dated set of tree-rings. Thus, the gaps between the dated elements are the gaps between the mid-points. The dating of the GEG-23A and GEG-24 samples encountered some unexplained laboratory issues. The first set of dates from Mannheim did not offer a successful wiggle-match. A re-run ("rev"=revised dates) of the samples and comparative dating of some samples at Heidelberg and at Arizona suggested more consistent but alternative dates. We have used these second run MAMS dates and the dates from Hd and AA in our model (excluded dates are indicated by the // notation before lines of code in Table S1). The pre-sequence wiggle-match dates are then cross-referenced later in the dating model. The wiggle-match date for sample TSA-14 from an I3a context, along with a historical tie point (see below), helps set a more precise date for this context where the radiocarbon dates on the other samples otherwise offer only wide possible date ranges given the plateau (the so-called Hallstatt plateau) in the radiocarbon calibration curve. For other uses of wiggle-matching to achieve greater calendar resolution within the Hallstatt plateau period, see, for example, Cook *et al*. (2010). The papers of Taylor & Southon (2010) and Jacobsson *et al*. (2018) highlight that the real situation, in detail, may be more complicated, with additional detailed shape and variation in the radiocarbon record evident at high-resolution across the Hallstatt plateau once we move beyond 10-year or 20-year tree-ring block 'averages' to, for example, annual values. Our TSA-14 wiggle-match fits radiocarbon measurements on 5-year 'blocks' (so 5-year averages) against the modelled 5-year values in IntCal13 (Reimer *et al*.

2013). We did this to match like with like. In the future, additional precision will be possible with an annual radiocarbon calibration curve.

(viii) The ArAGATS model begins with the "Sequence ("ArAGATS Model")" line of code. To assist the model to converge and run, the calendar range possible for the initial Boundary "Start of Sequence" is stated with uniform probability to lie somewhere between 3700 to 3200 BC. This date range was selected as reasonable but in no way influencing the calendar dating of the model since the earliest dates in the model offer calibrated ages at 95.4% probability (with no modelling), with earliest possible ranges from the 3600s–3300s BC.

(ix) All the Early Bronze Age (EBA) samples in the model are on charcoal samples unless stated otherwise. We note the material for all samples and sites in the LBA later part of the model where there are more elements and sites involved.

(x) Within the Phase "ArAGATS EBA and related" the various Sequences can float relative to each other. No order is assumed. The Aparan III and Karnut sets are included so as to compare their dates versus those for EB Gegharot. The Sequence "ArAGATS EB" inside this Phase is the archaeologically ordered (stratigraphic information) set of data from the excavations at Gegharot, comprising in general terms temporal relationships of Stratum 1a1 > Stratum 1a > 1a-b Transition Period > Stratum 1b. As noted in the comments (//), a few samples lacked clear contexts or assignments and a few assumed placements have been made.

(xi) The EB1-EB2 sequence at Gegharot ends before the middle of the third millennium BC. There is then no current evidence from the research of Project ArAGATS demonstrating occupation in the Tsaghkahovit Plain for over half a millennium. Two radiocarbon dates give age ranges indicating a Middle Bronze Age date. One was found in what was thought to be an EB context and the other in what was thought to be an Iron Age context (see AA-52899, AA-56976). They indicate some as yet unrecognised human presence in the area in the earlier second millennium BC. These two dates are placed in a Phase "MB presence". The samples were found respectively as intrusive in strata 1 and 3 contexts between the EBA and the LBA data.

(xii) A wood-charcoal sample (*Quercus* sp.) GEG-26A from a LBA midden likely offers an early Late Bronze Age (LBA) TPQ estimate (via a radiocarbon wiggle-match), and there is a solitary early LB1 date from Gegharot.

(xiii) The main ArAGATS LB1-2 Sequence follows. There are several site sequences that each float relative to each other. The site sets are placed, floating, within an overall Phase "later Late

Bronze 1 and 2 = Later Stratum 2a, 2b and 2 general charcoal". The aim is to clarify how these sites relate to each other in absolute time. At Gegharot, there are two strata, 2a and 2b, representing LB1 and LB2 (as the Label reading "T27 – 2b?" indicates, not everything is certain, but we have assumed that all the samples from this context are stratum 2b in addition to the end of 2b samples – the barley), but at the other sites, no stratigraphic definition was recognized during excavations, and the range of dates, for example, at Tsaghkahovit (Ar/Ts) indicates that the material dated covers both LB1 and LB2. At Gegharot, there are charcoal samples from stratum 2a and subsequent 2b, as well as a large set that could not be distinguished and is simply defined as stratum 2. In the main model these three groups were treated separately (floating versus each other) since the definition of 2a versus 2b was often problematic in the excavation. It seemed safest to treat these as perhaps (sometimes or partially) overlapping phases, letting the data place in relative terms, rather than stating as prior knowledge that they were definitely contiguous. In an alternative version of the model (Model 3a) the specific stratum 2a and 2b samples are placed in a site Sequence with 2a > 2b. (See the alternative code at the end of the main runfile. Note that the area where this code would replace the main code is indicated by the two comments in yellow highlight. These highlighted text comments are not part of the OxCal runfile). The relatively small differences in outcomes between these two approaches are listed in Table S2 and shown in Figure S1K. The one apparent exception is in the estimation of the dates and length for stratum 2a at Gegharot. If we assume a contiguous model, as in the alternative model, then this phase is noticeably longer. However, the dates for the surrounding phases do not change substantially.

(xiv) The end of the Ar/Ge Stratum 2b occupation is defined by the short-lived (barley) samples. The Tau_Boundary paired with a Boundary model on just the 5 barley dates in isolation run at the start of the model defined the Boundary for the end of this phase at 95.4 per cent probability as 1251–1093 BC. We used this range as the uniform total probability dating limits for the Boundaries demarcating the end of Ar/Ge stratum 2b and the Ar/Ge general stratum 2 phases. This is the only case among the four sites where we have short-lived sample material from an end of stratum 2 (or 2b) destruction context to provide a directly relevant date for these destructions. However, if we compare the other date estimates for stratum 2 or 2b contexts, or general stratum 1 and 2 contexts from charcoal samples (offering either TPQ estimates to approximate dates for these contexts) with the date estimates calculated for the subsequent

Boundaries *after* these contexts (thus a date for, or likely *terminus ante quem* for, the end of the relevant context), then we see that a likely or indicative date range for all the end of stratum 2b destructions at the four sites probably lies in the region *c*. 1220–1160 BC: Figure S3. These destructions need not of course all be approximately contemporary, but the evidence to hand would suggest they all likely occurred within a relatively brief period, and that they could in fact all be within a few years to a few decades of each other.

(xv) The Iron Age Sequence then follows in temporal terms: Iron 1a > Iron 1b > Iron 3 (there is no Iron 2 recognized so far) > Iron 4.

(xvi) The first stratum of post-Bronze Age date, the Iron 1a occupation at Gegharot, is labelled as stratum 2c as it appears to represent a late extension of the Late Bronze Age horizon rather than a new commitment to social life in the region. As noted in the labels for a few of the dated samples, they were moved from general stratum 2 to 2c assignments after post-excavation considerations of context and associated material (and consistent with the more recent radiocarbon dates). At Tsaghkahovit, some dates originally considered as stratum 2 and *late* Late Bronze Age have also been reassigned to Iron 1a, partly on the basis of reconsideration of the archaeology, and partly because the radiocarbon dates clearly support the Iron 1 dating of these samples/contexts. Thus, the archaeological assessments shaping strata assignments are not entirely independent of insights gleaned from the radiocarbon determinations in these cases. However, the observation that the overall project Bayesian chronological model runs successfully with good OxCal diagnostic statistic values supports these reassignments and the concomitant revised stratigraphic associations.

(xvii) The Iron 1b activity in the region was likewise recognized only post-excavation. At Tsaghkahovit this is a likely stratum 2d. The samples and radiocarbon dates were reassigned from original late stratum 2 assignments. At Aragatsi Berd (Ar/Ab) a similar stratum 2d was retrospectively recognized and some samples and radiocarbon dates were reassigned from original late stratum 2 assignments. These reassignments appear now to make sense in archaeological terms, but it is important to note that their stratum 2d assignment is not based on fully independent information. As with Iron 1a (above), the fact that the revised sequence is efficacious as part of an overall project Bayesian chronological model producing good OxCal diagnostic statistics provides grounds to support the reassignments and revised stratigraphic associations.

(xviii) The Iron 3 phase at Tsaghkahovit is recognized clearly from the archaeology and material culture (Khatchadourian 2008; 2014). Historical and archaeological assessment places the Iron 3a (I3a) Phase after 640 BC, the largely accepted date for the collapse of the Urartian Empire (Kroll 1984; Steele 2007; Zimansky 1995). On stylistic grounds, ceramic and other artefactual evidence from the site do not conclusively indicate occupation contemporary with the major Urartian fortress centres of the late ninth to mid seventh centuries BC. Moreover, the earliest diagnostic ceramic evidence associated with the middle Iron Age belongs to a regional pottery repertoire of the mid seventh to mid sixth centuries BC, which some scholars call the "Median Pottery Tradition" and others "late Urartian" (Khatchadourian in press; Kroll 2014; 2015). Finally, insofar as material assemblages from Urartian-era sites located beyond the Ararat Plain are often characterized by a preponderance of pottery belonging to a typological phase known as Lchashen-Metsamor 6 (Avetisyan & Avetisyan 2006), the scarcity of Lchashen-Metsamor 6 styles from floor deposits in the Iron 3 Tsaghkahovit settlement also favors a post–640 BC occupation. Independent confirmation of this archaeological-historical assessment comes from the dendroarchaeological sample TSA-14 (*Quercus* sp.). This sample provides a tree-ring sequenced wiggle-match date for the minimum date it was felled, taking the last extant tree-ring and allowing an approximate estimate for missing sapwood from what is clearly a relatively young tree, of 606–564 BC (68.2 per cent hpd) and 613-538 BC (95.4 per cent hpd). Since additional tree-rings could well be missing, this date is a minimum, the real felling date was likely at least a few years later, and thus likely around or after 600 BC. We assume this timber came from an architectural element in the I3a phase and so dates to the beginning/early part of the phase. Hence the TPQ of 640 BC that we imposed on archaeological-historical grounds is confirmed. We therefore employ a Calendar Date (C_Date) TPQ of 640 BC before this Phase in the model.

(xix) The Iron 3b (I3b) Phase follows. This phase is regarded on historical-archaeological criteria as post-540 BC. Charcoal samples belonging to this phase were collected in association with the latest discernible floor deposits (often flagstone floors), or in stratigraphic levels containing pottery forms that are diagnostic of the Achaemenid period (Khatchadourian in press). Hence a calendar date TPQ of 540 BC applies, an approximate date for the Achaemenid conquest of the Armenian highland (Khatchadourian 2008).

(xx) The later Iron 3b at Tsaghkahovit is specifically linked with the Achaemenid king Xerxes (Khatchadourian 2008). In particular, a floor context had the *in situ* presence of a serpentine plate that is very likely imported from the Persepolis area (based on form, as well as petrographic and chemical analysis). Many such serpentine and chert plates were found in the treasury at Persepolis, and some were inscribed. The Tsaghkahovit plate almost certainly does not pre-date the reign of Xerxes (486–465 BC). Hence the context of two samples linked to this floor is placed after Xerxes' accession, and thus after a TPQ of 486 BC. Another sample re-assigned to I3b post-excavation is not necessarily so closely associated with Xerxes and thus floats within an overall 13b Phase.

(xxi) The end of the Iron 3b phase concludes the main ArAGATS sequence. An Iron 4 Phase is recognized based on the radiocarbon date of a sample from Gegharot and is contemporary with the Roman period. A subsequent "Medieval" phase is recognized from the date of a sample from Tsaghkahovit. Finally, a wood-charcoal sample (GEG-25A) recovered from Gegharot was dated and, unexpectedly, found to belong to the later second millennium AD. This wiggle-match ends the ArAGATS sequence. The End of Sequence Boundary is constrained based on the known information with a uniform probability between AD 1000–2000.

(xxii) The last lines of the runfile cross reference earlier parameters and calculate an approximate overall timespan for the Late Bronze 1-2 in the ArAGATS sequence, and run correlations of the dating probabilities for Gegharot stratum 1a1 and 1a against the dates from Aparan III and Karnut (Figure 2): see Figures. S4-S7.

(xxiii) Finally, it is important to highlight that in a large and complicated model such as this, different runs of the model will yield very slightly varying results, especially for the less well constrained or defined elements. Where the objects are well defined (i.e., elements like the wiggle-matches) more or less the same result will be found repeatedly. Where there are a number of data in a clear structure, then again, there is usually only very small variation over several runs (typically of the low single digit range). But where there are few data and only looser or loose constraints, then somewhat larger variations are possible between different runs. We report data that is typical from runs that completed, with satisfactory Amodel and Aoverall values, and where all data have individual convergence values greater than 95 (in the case of Model 3 all were consistently >99) (Bronk Ramsey 2009a).

We show a summary of Model 3, indicating the 95.4 per cent probability calendar age ranges for the main elements, against (i) the approximate 95.4 per cent probability overall calendar age ranges for the elements dated in Cherry *et al*. (2007) from the Vorotan Project in southern Armenia, and (ii) the 68.2 per cent ranges for the overall Kura-Araxes II span ('Interval' method) determined by Passerini *et al*. (2016) from the site of Aradetis Orgora in Georgia, in Figure S8. The Kura-Araxes II date range determined from Aradetis Orgora in Georgia is largely similar to the range found from the available EB ArAGATS samples. Our ArAGATS sequence lacks any clear Middle Bronze Age data, in contrast to the Vorotan Project in southern Armenia. Conversely, the Vorotan Project did not locate any Late Bronze Age, in marked contrast to the ArAGATS project. The early Iron Age of the Vorotan Project at Uits (starting in the twelfth century BC) would almost directly follow the close of the LBA among the ArAGATS sites. The remainder of the Iron Age sequence from the Vorotan Project is less well defined but appears largely contemporary with parts of the ArAGATS sequence. However, it also includes the post-Achaemenid elements in the third century BC to second century AD, which are not recognized so far by Project ArAGATS.

In Figure S9 we show the early Middle Bronze Age (MBA) dates from several sites presented in Sagona (2017: 302). The single date on a wood (*Quercus sp*.) sample from Martkopi Barrow 4 (Wk-35425), in particular, suggests that the initial MBA may reach back within *c*. 200–320 years (68.2 per cent probability) or 124–384 years (95.4 per cent probability) of the current modelled end of EBA Gegharot 1b (Figures 2, S1, Table S2) (even trying to allow a little for in-built age in this oak sample—but assuming it is not residual wood or inner rings from a very old oak tree): see Figure S10. It is not clear on the currently available evidence how this 'gap' is (or is not) filled, and especially whether the EBA should extend further – although one date from Gegharot might hint at this possibility (see (v) above). The other dates in Figure S9 indicate that parts of the earlier MBA range across the period from the twenty fifth to twenty third centuries BC.

In Figure S11 we add a comparison with the radiocarbon dates reported from the sites of Chobareti (Kakhiani *et al*. 2013; Sagona 2014) in southern Georgia and Sos Höyük VA in eastern Turkey (Sagona 2014) against the early EBA Project ArAGATS dates and for those other sites from the immediate area (Aparan III, Karnut), thus expanding the data shown in Figures 2

and S1. We employ the same methods as in Model 3 (thus Charcoal Plus Outlier model for the dates on charcoal samples and the General Outlier model for the dates on shorter/short-lived samples). The Chobareti and Sos Höyük data are treated each as an independent Sequence and Phase that overlaps with the other EBA data. Note, for date Wk-34451 from Chobareti, we employ the measurement error of ±30 in Kakhiani *et al*. (2013) – the ±90 in Sagona (2014: Table 2) appears to be a typo; and, for the date Beta-120452 Sos Höyük, we employ an error of ±50 from (http://www.tayproject.org/C14.fm$Retrieve?YerlesmeNo=2407&html=C14Detail.html&layout=web) since Sagona (2014: Table 3 has a typo and is missing the "5"). The Chobareti data overall indicate a calendar date range for the site of 3281–3216 BC (26.2 per cent) and 3181–3086 BC (42 per cent) at 68.2 per cent probability and 3323–3046 BC at 95.4 per cent probability. This means the site likely overlaps with the initial stratum 1a1 at Gegharot and with Karnut, and is earlier than Gegharot stratum 1a (2997–2913 BC at 68.2 per cent probability and 3007–2906 BC at 95.4 per cent probability: Table S2) and much of Aparan III. The Sos Höyük VA data overall indicate a calendar date range for the site phase of 3306–3036 BC at 68.2 per cent probability and 3430–2907 BC at 95.4 per cent probability. This means that Sos Höyük VA also likely overlaps with the initial stratum 1a1 at Gegharot and with Karnut, and is largely earlier than both Gegharot stratum 1a (at most its very final years might almost overlap with the start of Gegharot stratum 1a) and also much of Aparan III.

References

ASHMORE, P.J. 1999. Radiocarbon dating: avoiding errors by avoiding mixed samples. *Antiquity* 73: 124–30. https://doi.org/10.1017/S0003598X00087901

AVETISYAN H.G. & P.S. AVETISYAN. 2006. *Araratyan dashti mshakuyte M.T.A. XI-VI darerum*. Yerevan: Yerevan State University.

BADALYAN, R., A.T. SMITH, I. LINDSAY, L. KHATCHADOURIAN & P. AVETISYAN. 2008. Village, fortress, and town in Bronze and Iron Age Southern Caucasia: a preliminary report on the 2003-2006 investigations of Project ArAGATS on the Tsaghkahovit Plain, Republic of Armenia. *Archäologische Mitteilungen aus Iran und Turan* 40: 45–105.

BADALYAN, R., A.T. SMITH, I. LINDSAY, A. HARUTYUNYAN, A. GREENE, M. MARSHALL, B. MONAHAN & R. HOVSEPYAN. 2014. A preliminary report on the 2008, 2010, and 2011

investigations of Project ArAGATS on the Tsaghkahovit Plain, Republic of Armenia. *Archäologische Mitteilungen aus Iran und Turan* 46: 149–222.

BADALYAN, R.S., A.T. SMITH, L. KHATCHADOURIAN. 2010. Project ArAGATS: 10 years of investigations into Bronze and Iron Age sites in the Tsaghkahovit Plain, Republic of Armenia. *TÜBA-AR* 13: 264–76.

BAYLISS, A., J. VAN DER PLICHT, C. BRONK RAMSEY, G. MCCORMAC, F. HEALY & A. WHITTLE. 2011. Towards generational time-scales: the quantitative interpretation of archaeological chronologies, in A. Whittle, F. Healy & A. Bayliss (ed.), *Gathering time: dating the Early Neolithic enclosures of southern Britain and Ireland*: 17–59. Oxford: Oxbow Books.

BOARETTO, E. 2015. Radiocarbon and the archaeological record: an integrative approach for building an absolute chronology for the Late Bronze and Iron Ages of Israel. *Radiocarbon* 57(2): 207–16. https://doi.org/10.2458/azu_rc.57.18554

BRONK RAMSEY, C. 1995. Radiocarbon calibration and analysis of stratigraphy: the OxCal program. *Radiocarbon* 37(2): 425–30. https://doi.org/10.1017/S0033822200030903

BRONK RAMSEY, C. 2009a. Bayesian analysis of radiocarbon dates. *Radiocarbon* 51(1): 337–60. https://doi.org/10.1017/S0033822200033865

BRONK RAMSEY, C. 2009b. Dealing with outliers and offsets in radiocarbon dating. *Radiocarbon* 51(3): 1023–45. https://doi.org/10.1017/S0033822200034093

BRONK RAMSEY, C., M.W. DEE, J.M. ROWLAND, T.F.G. HIGHAM, S.A. HARRIS, F. BROCK, A, QUILES, E.M. WILD, E.S. MARCUS & A.J. SHORTLAND. 2010. Radiocarbon-based chronology for Dynastic Egypt. *Science* 328: 1554–57.

BRONK RAMSEY, C., J. VAN DER PLICHT & B. WENINGER. 2001. 'Wiggle matching' radiocarbon dates. *Radiocarbon* 43(2A): 381–89. https://doi.org/10.1017/S0033822200038248

CHERRY J., S. MANNING, S. ALCOCK, A. TONIKYAN & M. ZARDARYAN. 2007. Radiocarbon dates for the second and first millennia BC from southern Armenia: preliminary results from the Vorotan Project (2005–2006). *ARAMAZD* (Armenian Journal of Near Eastern Studies) 2: 52–71.

COOK, G.T., T.N. DIXON, N. RUSSELL, P. NAYSMITH, S. XU & B. ANDRIAN. 2010. High-precision radiocarbon dating of the construction phase of Oakbank Crannog, Loch Tay, Perthshire. *Radiocarbon* 52(2–3): 346–55. https://doi.org/10.1017/S0033822200045392

DEE, M. & C. BRONK RAMSEY, C. 2014. High-precision Bayesian modelling of samples susceptible to inbuilt age. *Radiocarbon* 56(1): 83–94. https://doi.org/10.2458/56.16685

DEE, M., D. WENGROW, A. SHORTLAND, A. STEVENSON, F. BROCK, L.G. FLINK & C. BRONK RAMSEY. 2013. An absolute chronology for early Egypt using radiocarbon dating and Bayesian statistical modelling. *Proceedings of the Royal Society* A 469: 20130395. https://doi.org/10.1098/rspa.2013.0395

GALIMBERTI, M., BRONK RAMSEY, C. & S.W. MANNING. 2004. Wiggle-match dating of tree ring sequences. *Radiocarbon* 46(2): 917–24. https://doi.org/10.1017/S0033822200035967

HANECA K, K. ČUFAR & H. BEECKMAN. 2009. Oaks, tree-rings and wooden cultural heritage: a review of the main characteristics and applications of oak dendrochronology in Europe. *Journal of Archaeological Science* 36: 1–11. https://doi.org/10.1016/j.jas.2008.07.005

HIGHAM, T., R. WARREN A. BELINSKIJ & H. HÄRKE. 2010. Radiocarbon dating, stable isotope analysis, and diet-derived offsets in ^{14}C ages from the Klin-Yar site, Russian North Caucasus. *Radiocarbon* 52(2–3): 653–70. https://doi.org/10.1017/S0033822200045689

JACOBSSON, P., W.D. HAMILTON, G. COOK, A. CRONE, E. DUNBAR, H. KINCH, P. NAYSMITH, B. TRIPNEY & S. XU. 2018. Refining the Hallstatt Plateau: short-term ^{14}C variability and small scale offsets in 50 consecutive single tree-rings from southwest Scotland dendro-dated to 510–460 BC. *Radiocarbon* 60(1): 219–37. https://doi.org/10.1017/RDC.2017.90

JUDE F, M. MARGUERIE, R. BADALYAN, A.T. SMITH & A. DELWAIDE. 2016. Wood resource management based on charcoals from the Bronze Age site of Gegharot (central Armenia). *Quaternary International* 395: 31–44. https://doi.org/10.1016/j.quaint.2015.04.019

KAKHIANI, K., A. SAGONA, C. SAGONA, E. KVAVADZE, G. BEDIANASHVILI, E. MASSAGER, L. MARTIN, E. HERRSCHER, I. MARTKOPLISHVILI, J BIRKETT-REES & C. LONGFORD. 2013. Archaeological investigations at Chobareti in southern Georgia, the Caucasus. *Ancient Near Eastern Studies* 50: 1–138.

KHATCHADOURIAN, L. 2014. Empire in the everyday: a preliminary report on the 2008–2011 excavations at Tsaghkahovit, Armenia. *American Journal of Archaeology* 118: 137–69. https://doi.org/10.3764/aja.118.1.0137

– 2008. Social logics under empire: the Armenian ‘Highland Satrapy’ and Achaemenid Rule, ca. 600–300 BC. Ph.D. dissertation, University of Michigan.

– In press. Pottery typology and craft learning in the northern Near East.” *Iranica Antiqua*.

KROLL, S. 1984. Urartus Untergang in anderer Sicht (La chute de l’Urartu: Une autre vue). *Istanbuler Mitteilungen* 34: 151–70.

– 2014. Notes on the post-Urartian (median) horizon in NW-Iran and Armenia, in A. Özfırat (ed.) *Arkeolojiyle Geçen Bir Yaşam Için Yazılar: Veli Sevin'e Armağan: Scripta*: 203–10. Istanbul: Yayınları.
– 2015. Archaeology between Urartu and the Achaemenids, in M. Işikli and B. Can (ed.) *Uluslararası Doğu Anadolu Güney Kafkasya Kültürleri Sempozyumu*: 110–17. Newcastle: Cambridge Scholars Press.
PASSERINI, A., L. REGEV, E. ROVA & E. BOARETTO. 2016. New radiocarbon dates for the Kura-Araxes occupation at Aradetis Orgora, Georgia. *Radiocarbon* 58(3): 649–77. https://doi.org/10.1017/RDC.2016.37
PHILIPPSEN, B. 2013. The freshwater reservoir effect in radiocarbon dating. *Heritage Science* 1: 24. https://doi.org/10.1186/2050-7445-1-24
REIMER, P.J., *et al*. 2013. IntCal13 and Marine13 radiocarbon age calibration curves 0–50,000 years cal BP. *Radiocarbon* 55: 1869–87. https://doi.org/10.2458/azu_js_rc.55.16947
SAGONA, A. 2014. Rethinking the Kura-Araxes genesis. *Paléorient* 40(2): 23–46. https://doi.org/10.3406/paleo.2014.5634
– 2017. *The archaeology of the Caucasus from earliest settlements to the Iron Age*. Cambridge: Cambridge University Press.
SMITH, A.T., R. BADALYAN, P. AVETISYAN & M. ZARDARYAN. 2004. Early complex societies in Southern Caucasia: a preliminary report on the 2002 investigations by Project ArAGATS on the Tsakahovit Plain, Republic of Armenia. *American Journal of Archaeology* 108: 1–41. https://doi.org/10.3764/aja.108.1.1
SMITH, A.T., R.S. BADALYAN, P. AVETISYAN, A. GREENE & L. MINC. 2009. *The archaeology and geography of ancient Transcaucasian societies. Volume 1: the foundations of research and regional survey in the Tsaghkahovit Plain, Armenia* (Oriental Institute Publications Volume 134). Chicago: The Oriental Institute of the University of Chicago.
STEELE, L. 2007. Urartu and the Medikos Logos of Herodotus. *American Journal of Ancient History* 2.2: 5–16.
TAYLOR R.E. & J. SOUTHON. 2013. Reviewing the mid-first millennium BC ^{14}C "warp" using ^{14}C bristlecone pine data. *Nuclear Instruments and Methods in Physics Research B* 294: 440–43. https://doi.org/10.1016/j.nimb.2012.08.057

WARD G.K. & S.R. WILSON. 1978. Procedures for comparing and combining radiocarbon age determinations: a critique. *Archaeometry* 20: 19–31. https://doi.org/10.1111/j.1475-4754.1978.tb00208.x

WATERBOLK, H.T. 1971. Working with radiocarbon dates. *Proceedings of the Prehistoric Society* 37: 15–33. https://doi.org/10.1017/S0079497X00012548

ZIMANSKY, P. 1995. Xenophon and the Urartian Legacy, in P. Briant (ed.) *Dans les pas des Dix-Mille: peuples et pays du Proche-Orient vus par un Grec*: 255–68. Toulouse: Presses universitaires du Mirail.

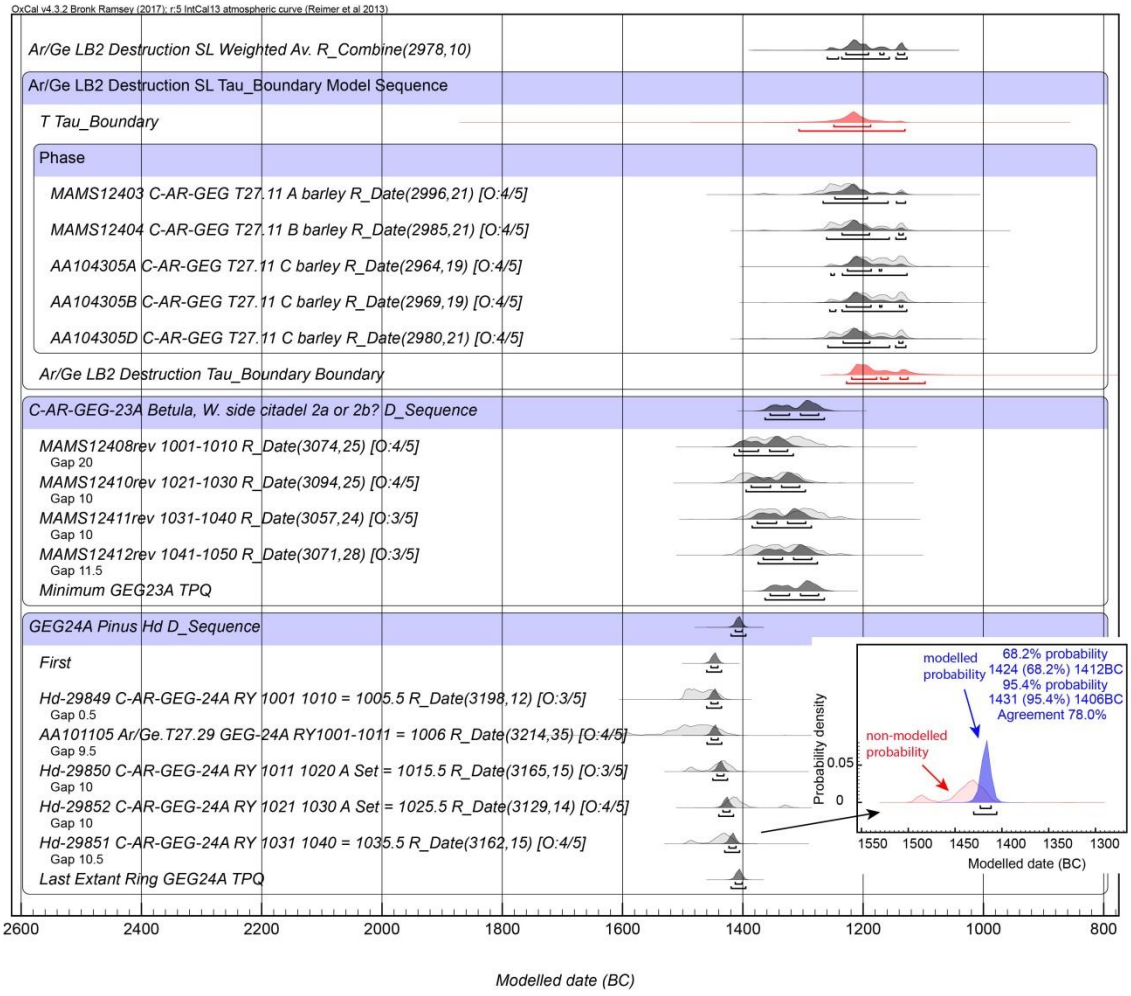

Figure S1. A. (continued in Figures S1 B to S1 J) Whole ArAGATS Model 3 output – the main model from Table S1 runfile. The black/grey, red, green and orange histograms represent the modelled calendar dating probabilities. The light grey histograms show the non-modelled calendar dating probabilities for individual radiocarbon dates; the smaller dark gray/black histograms show the modelled calendar probability (see Figure S1 A INSET where red = non-modelled [i.e. light grey], and blue = modelled [i.e. dark grey/black] for radiocarbon date Hd-29851 as an illustration). The upper and lower lines under each modelled distribution respectively indicate the 68.2 per cent highest posterior density (hpd) and 95.4 per cent hpd ranges. The red, orange and green distributions show elements calculated from the model. Boundaries represent the periods of time delimiting the groupings of dates – with the exception of the single instance of a Tau_Boundary paired with a Boundary giving an exponential distribution, all the other groups of data are assumed to be events randomly sampled from a uniform distribution. Boundaries are shown in red. The probability density functions shown in

green are from Date queries where the Date command calculates a date probability function for the given element as constrained by the model – in each case in our model as an estimate for an entire Phase. Thus the Date Estimate Stratum 1a in Figure S1 C is a probability distribution for the date of Stratum 1a from the whole of the modelled evidence for this stratum. The two orange distributions are where a Boundary is estimating the (relatively long) period of time between the adjacent elements of the model. Figures S1C-I overlap by one element in each case.

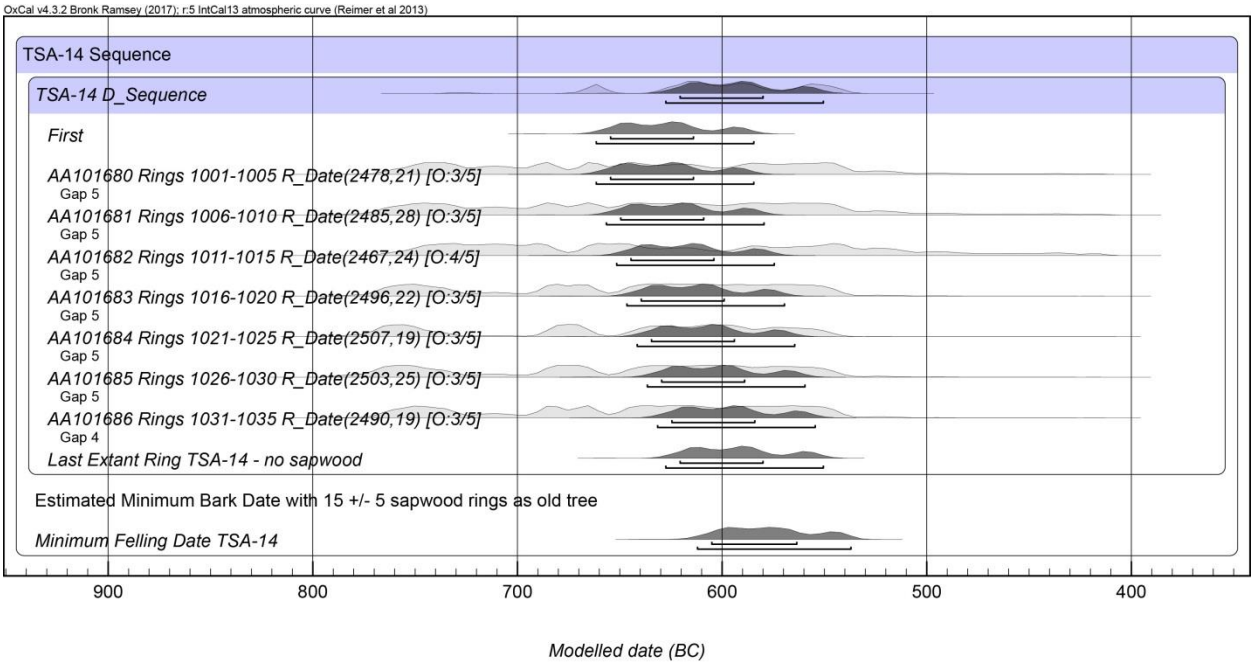

Figure S1. B. Continuation of Figure S1A.

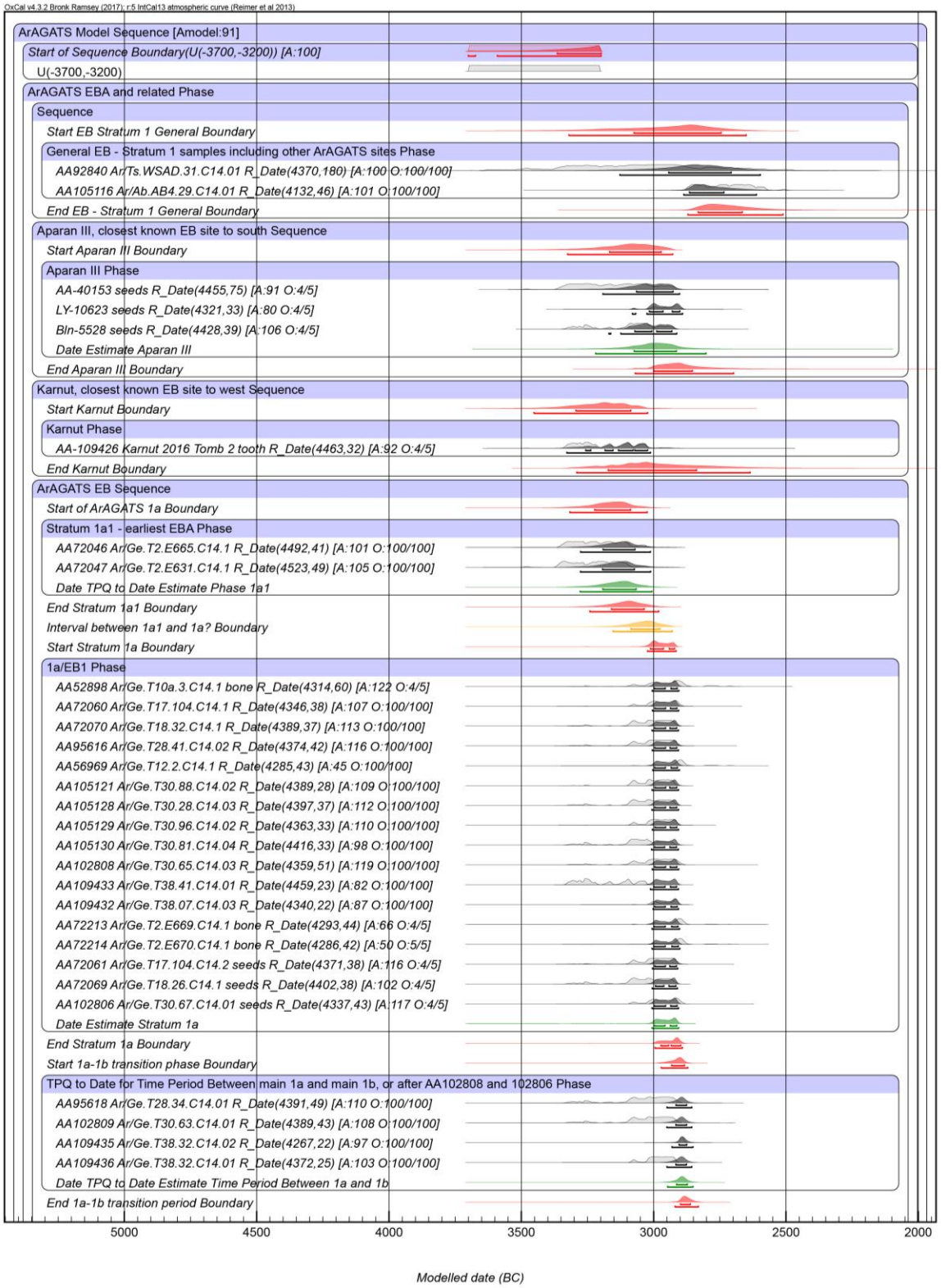

Figure S1. C. Continuation of Figure S1A. This and subsequent plots though to Figure S1 I overlap at the starts/ends of each plot shown.

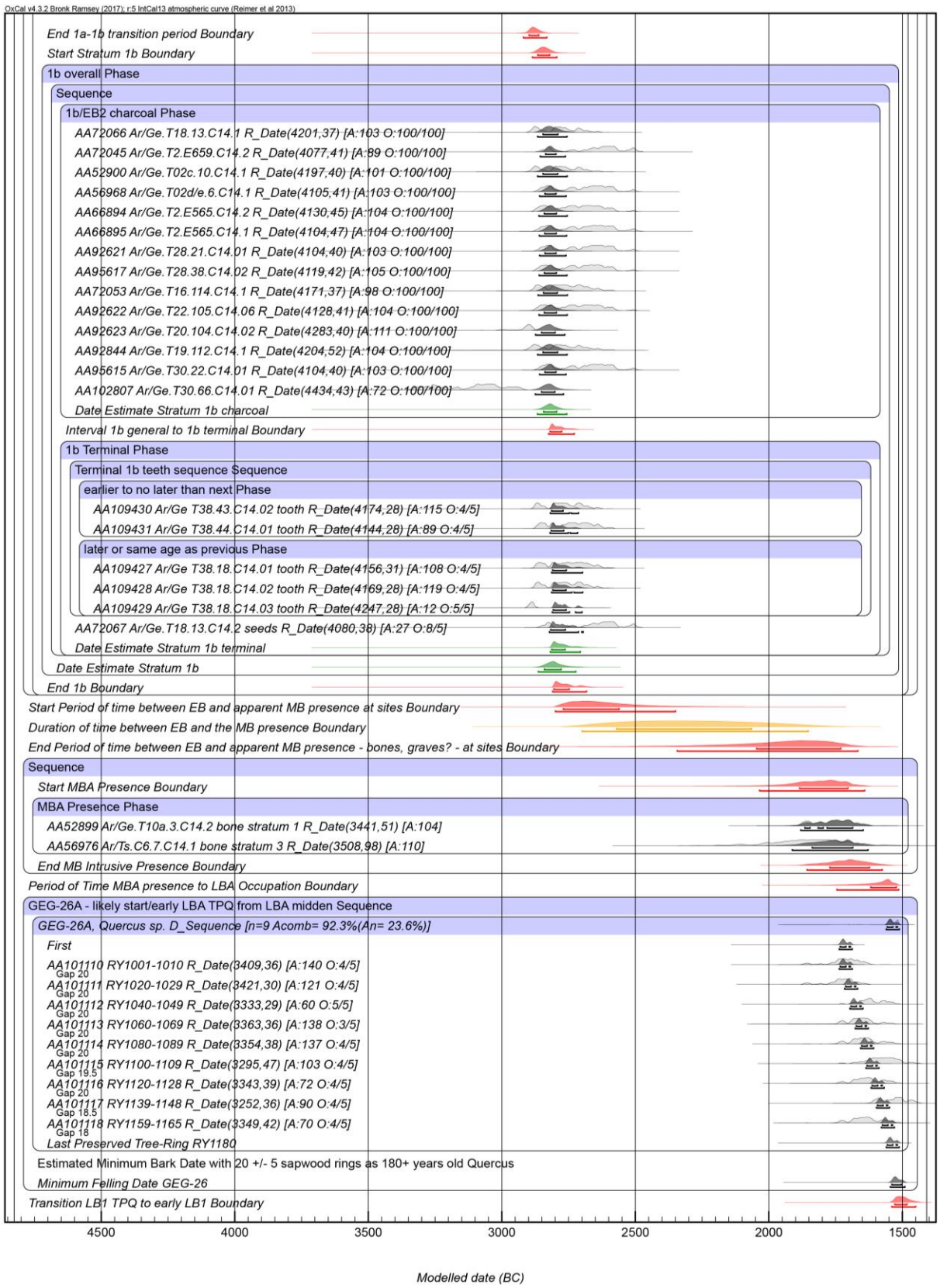

Figure S1. D. Continuation of Figure S1A.

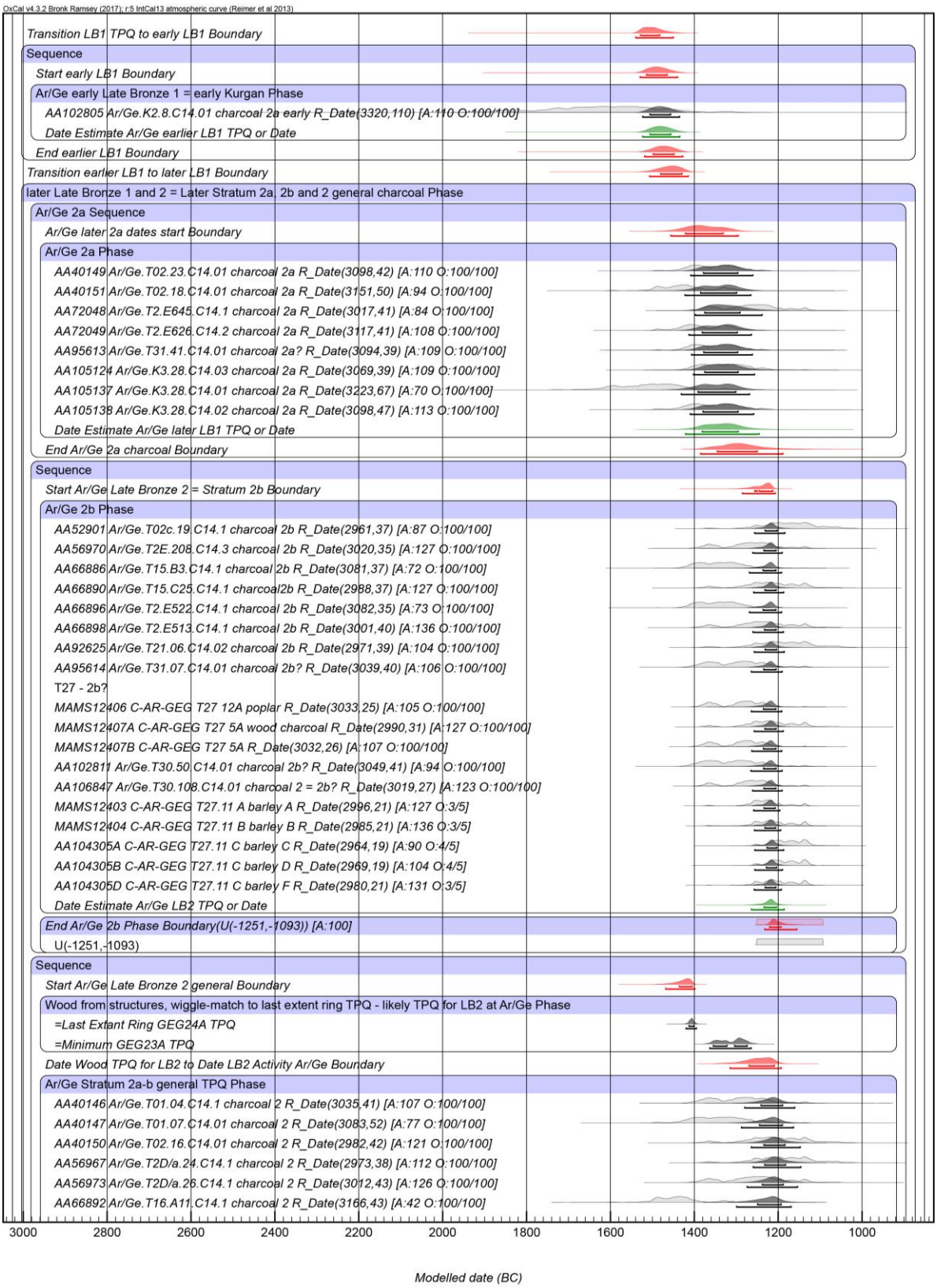

Figure S1. E. Continuation of Figure S1A.

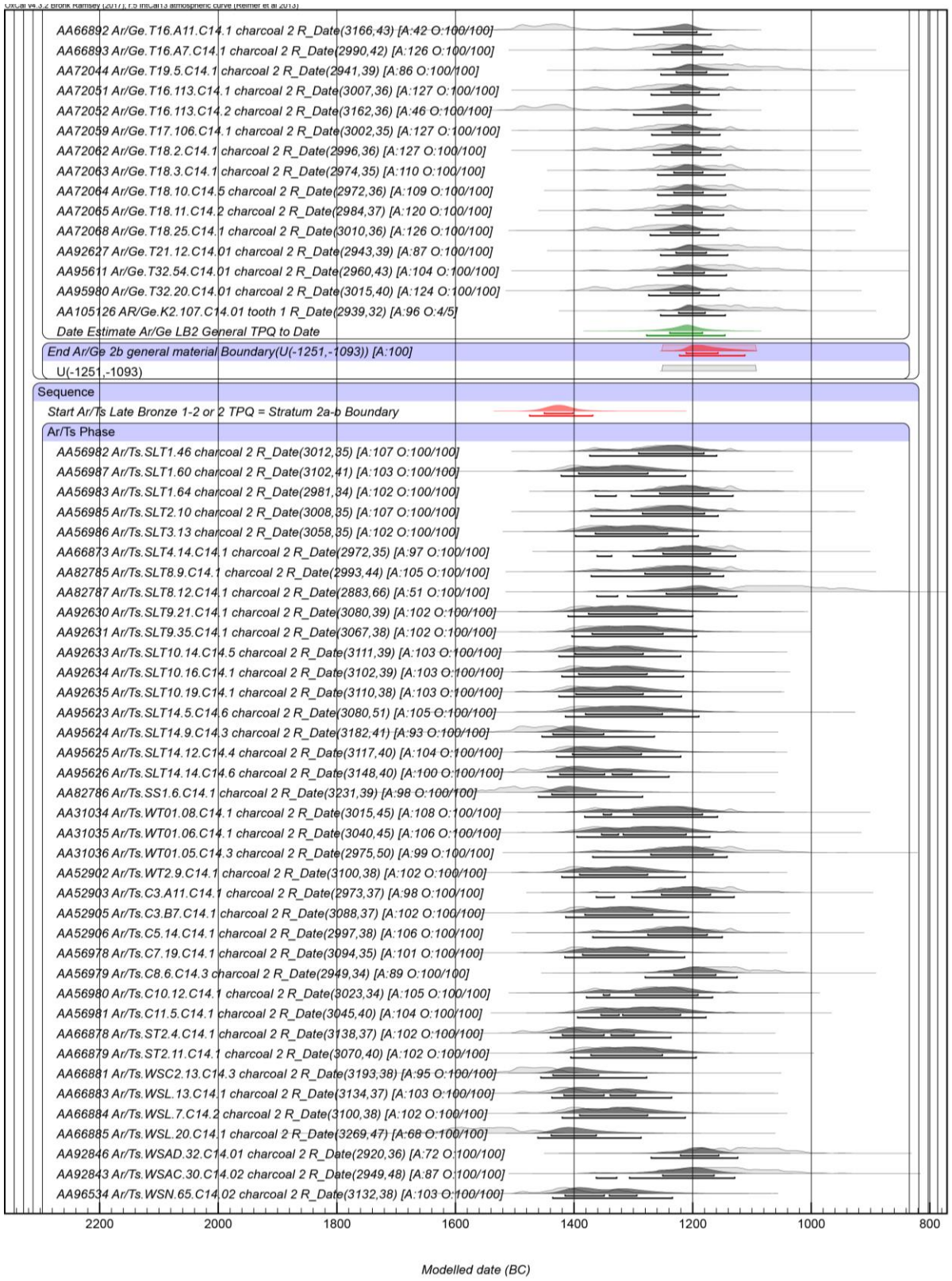

Figure S1. F. Continuation of Figure S1A.

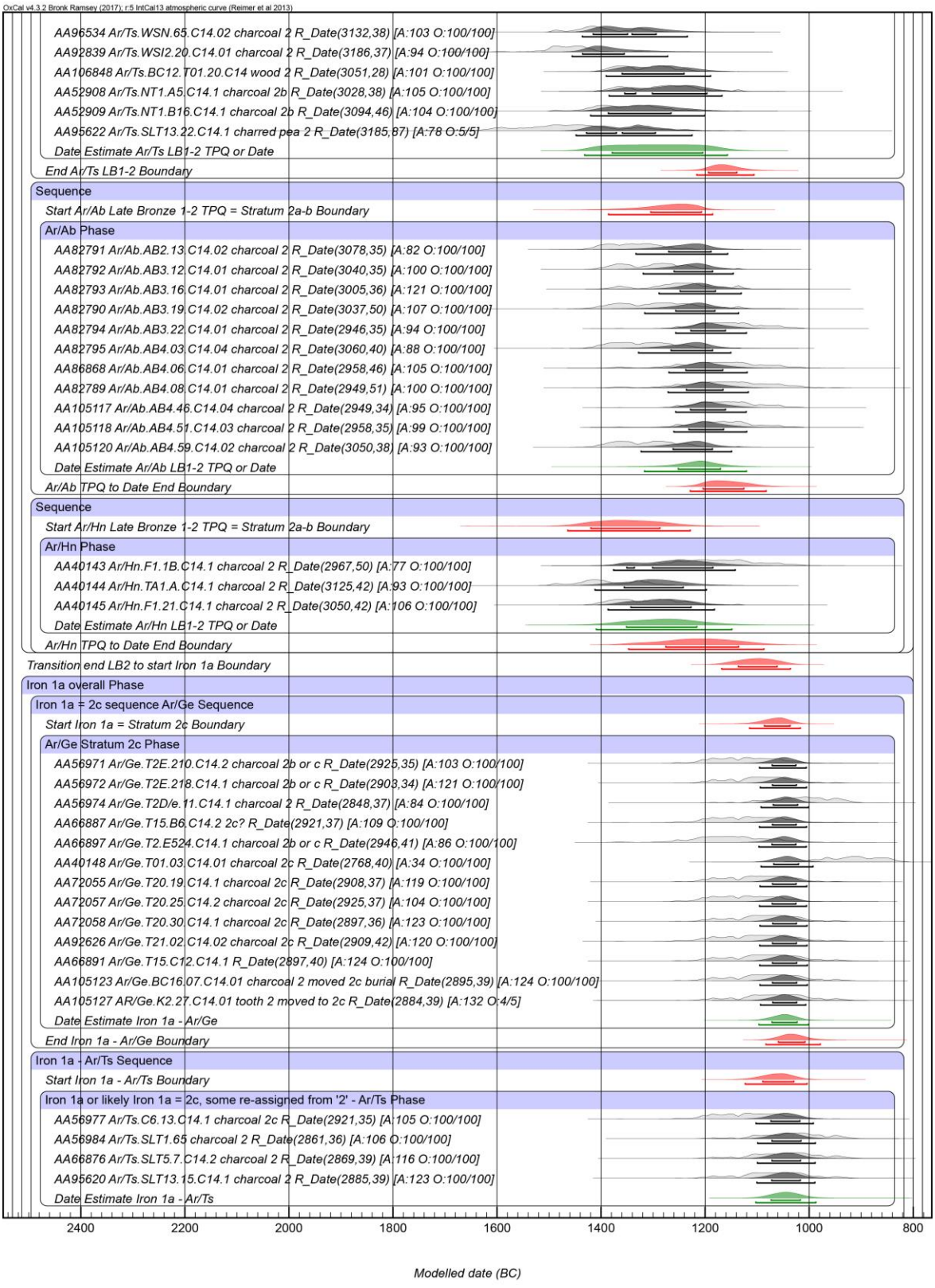

Figure S1. G. Continuation of Figure S1A.

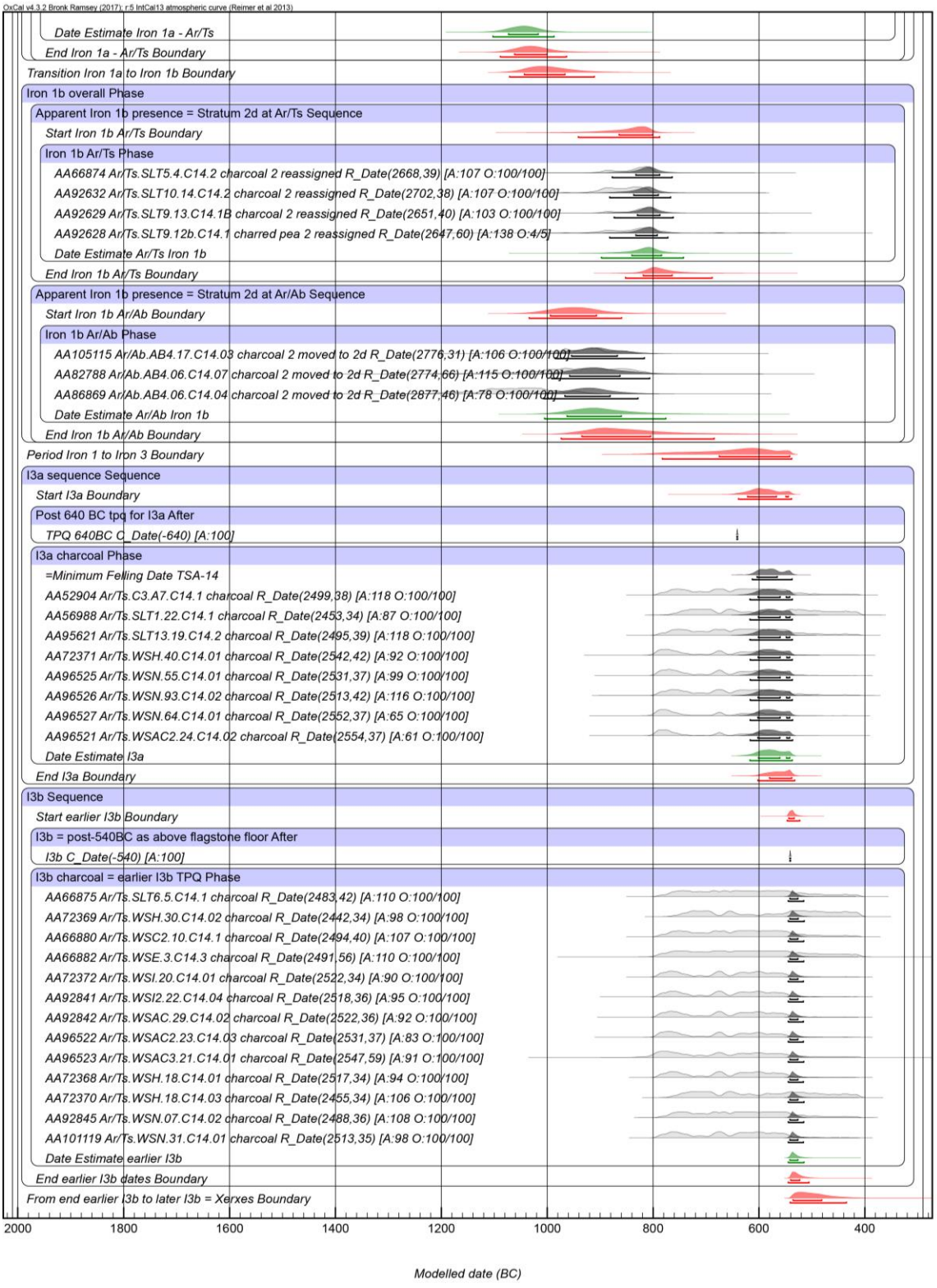

Figure S1. H. Continuation of Figure S1A.

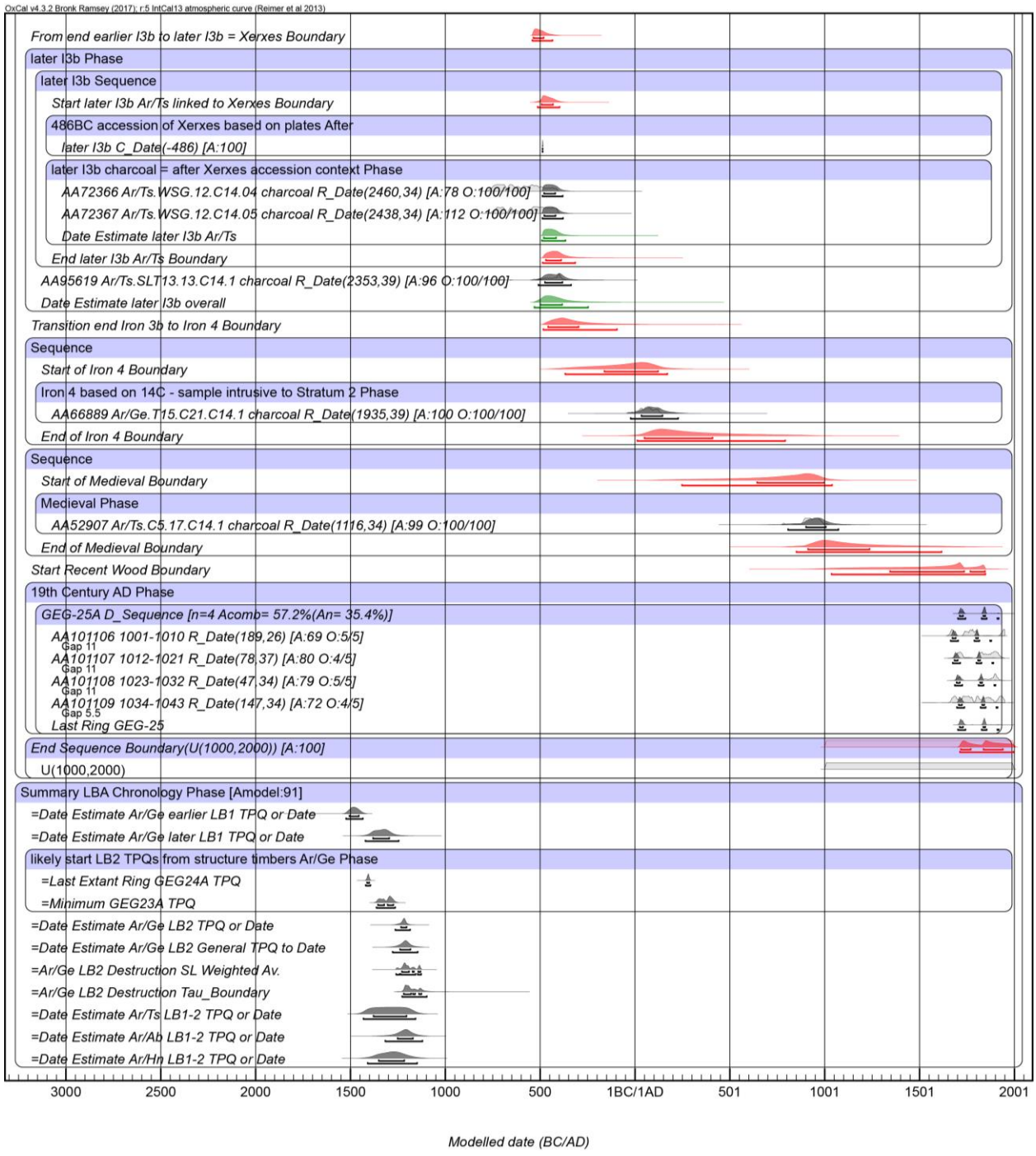

Figure S1. I. Continuation of Figure S1A.

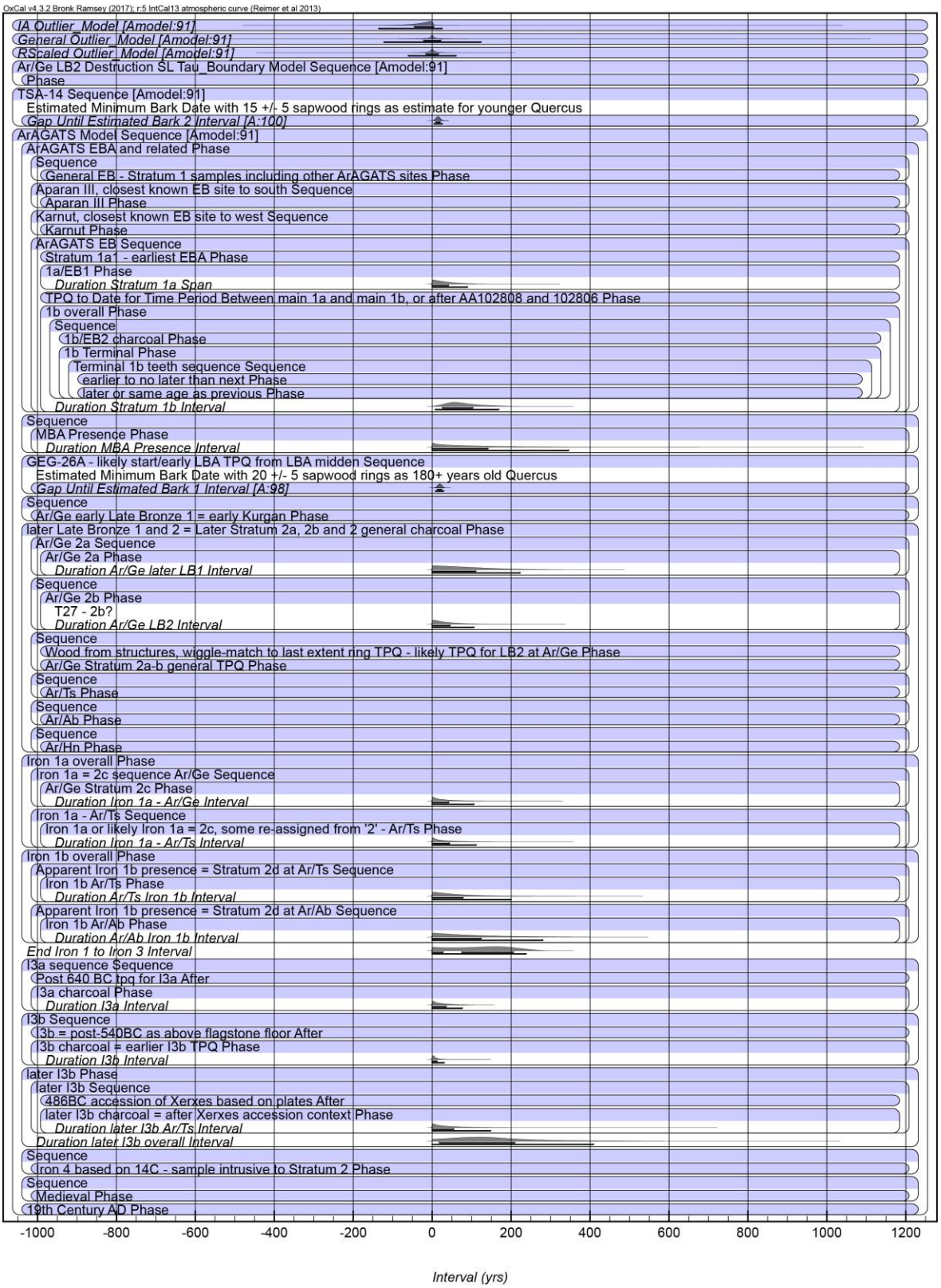

Figure S1. J. Model structure and elements and Intervals from Model 3 (as shown Figure S1A-I).

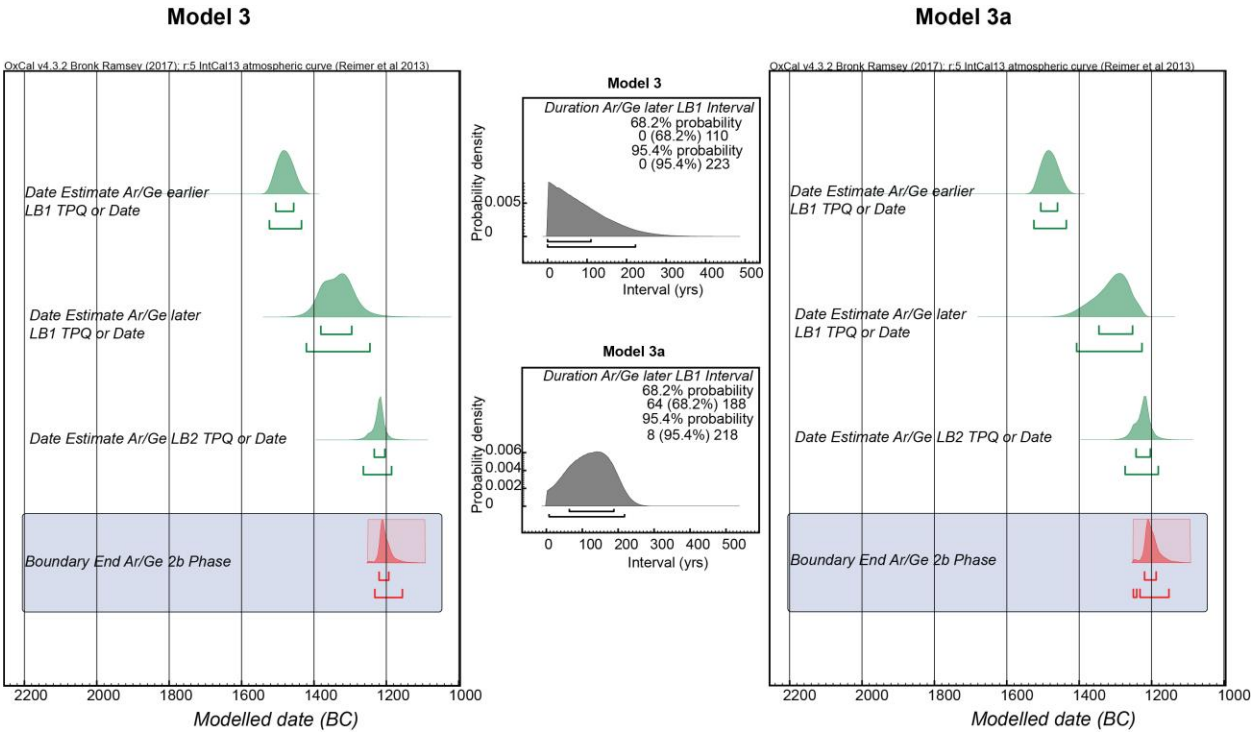

Figure S1. K. Comparison of Model 3 versus Model 3a results (see also Table S2) for the part of the model with alternative code in Model 3a (see OSM text, Table S1). The only substantive difference, contrasting potentially overlapping versus contiguous 2a and 2b strata at Gegharot, concerns the likely duration (length) of the later LB1 interval.

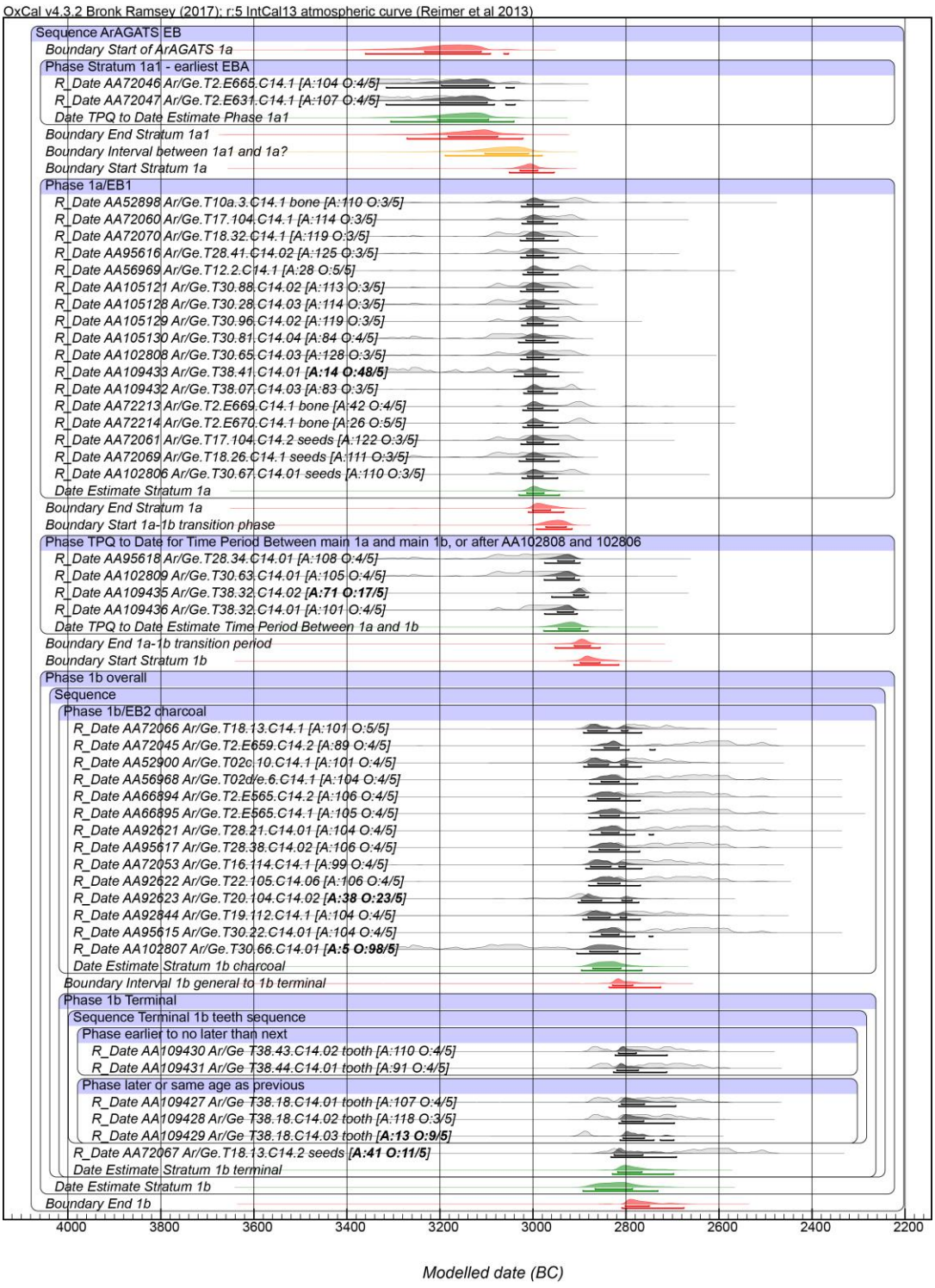

Figure S2 A. Model 1 (the model in Table S1 = Model 3 but with all the non-wiggle-match charcoal samples considered applying the General Outlier model, versus using the Charcoal Plus Outlier model). See discussion in (i) (a)–(c) above. Outliers indicated in bold. EBA portion of Model 1 is shown.

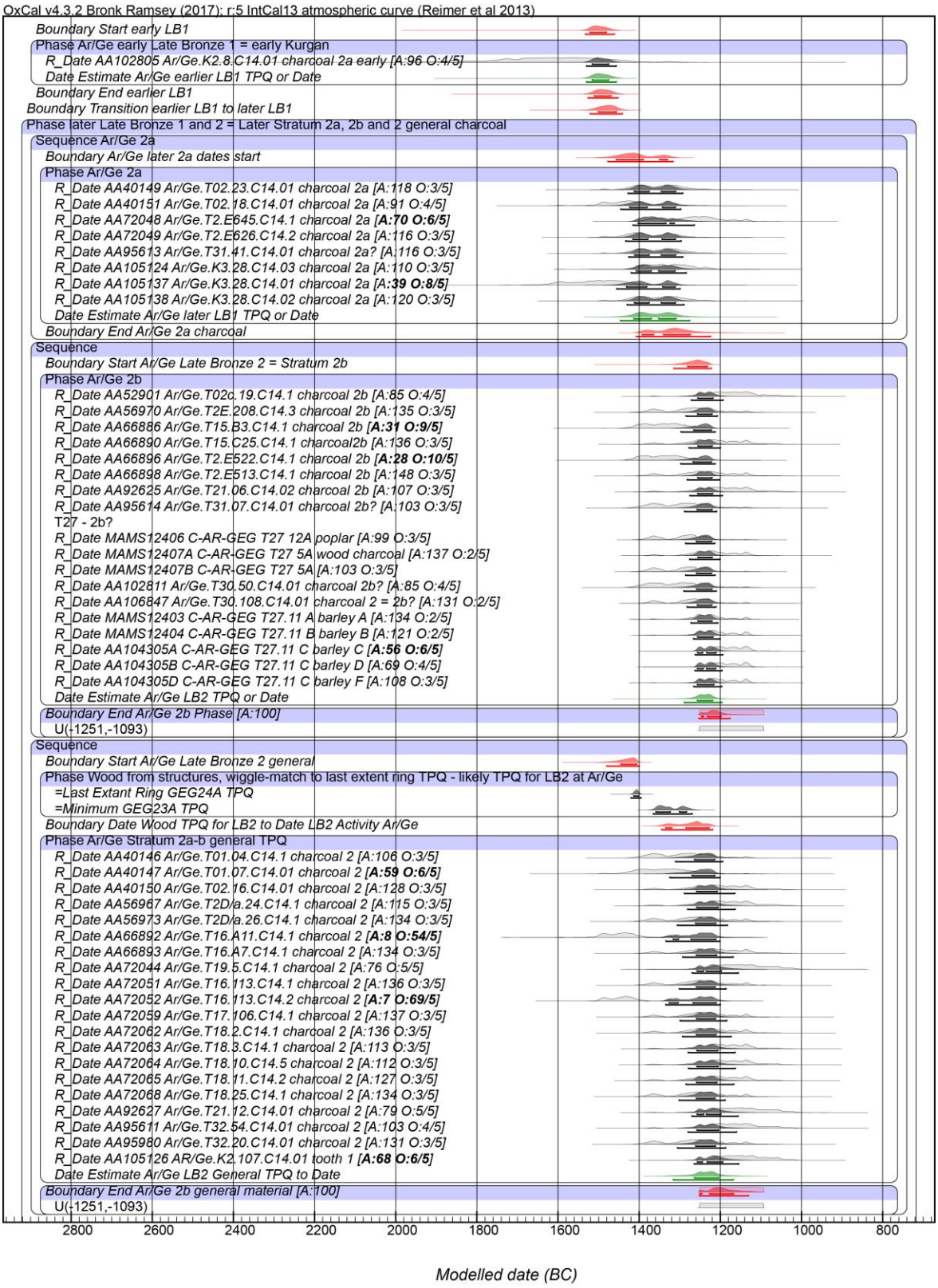

Figure S2 B. Model 1 continued from Figure S2 A. First part of the LBA sequence is shown (remainder of LBA in Figure S2 C).

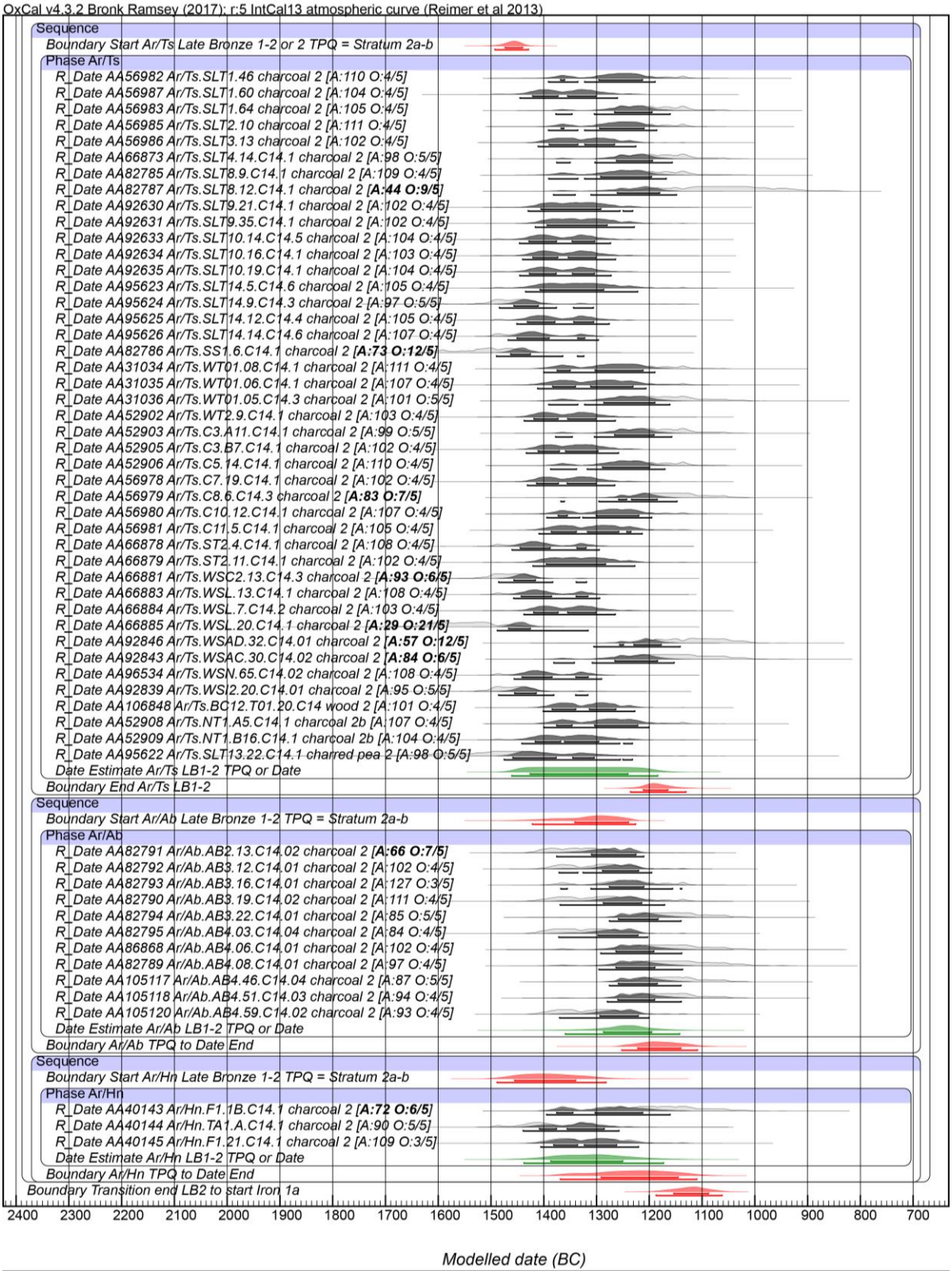

Figure S2 C. Model 1 continued from Figure S2 B. Second part of the LBA sequence is shown.

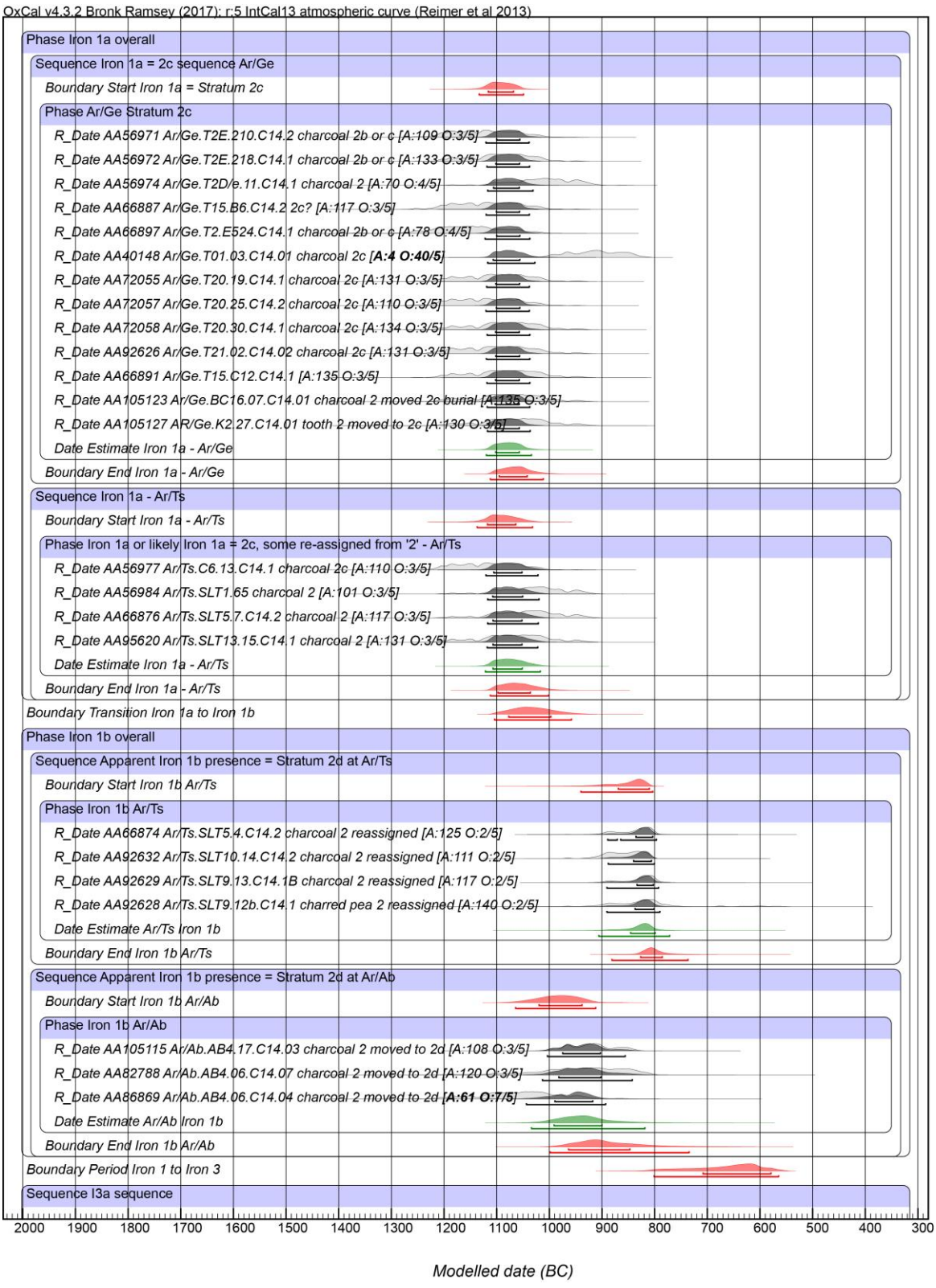

Figure S2 D. Model 1 continued from Figure S2 C. First part of the Iron Age sequence is shown (remainder of the Iron Age in Figure S2 E).

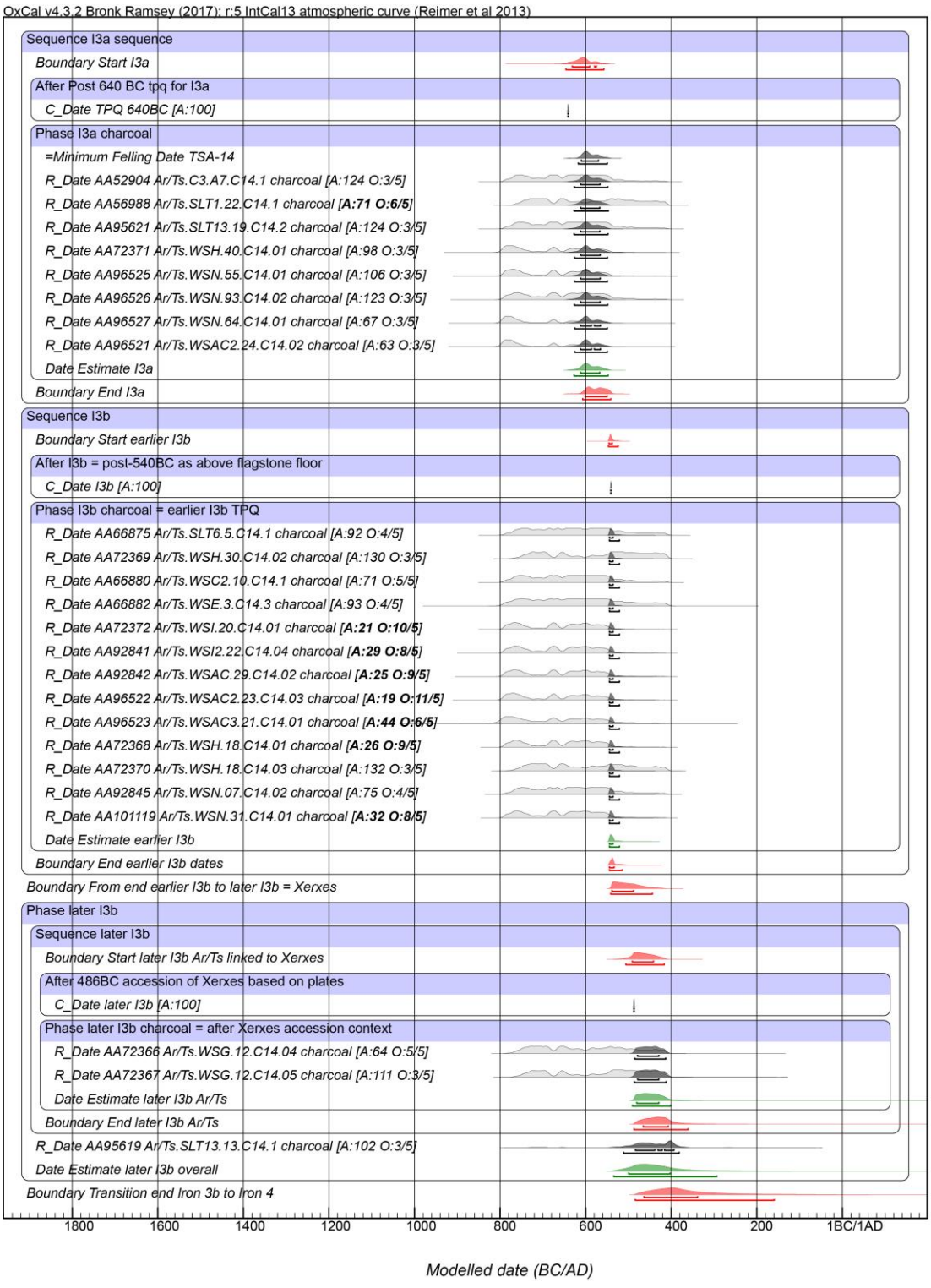

Figure S2 E. Model 1 continued from Figure S2 D. Second part of the Iron Age sequence is shown.

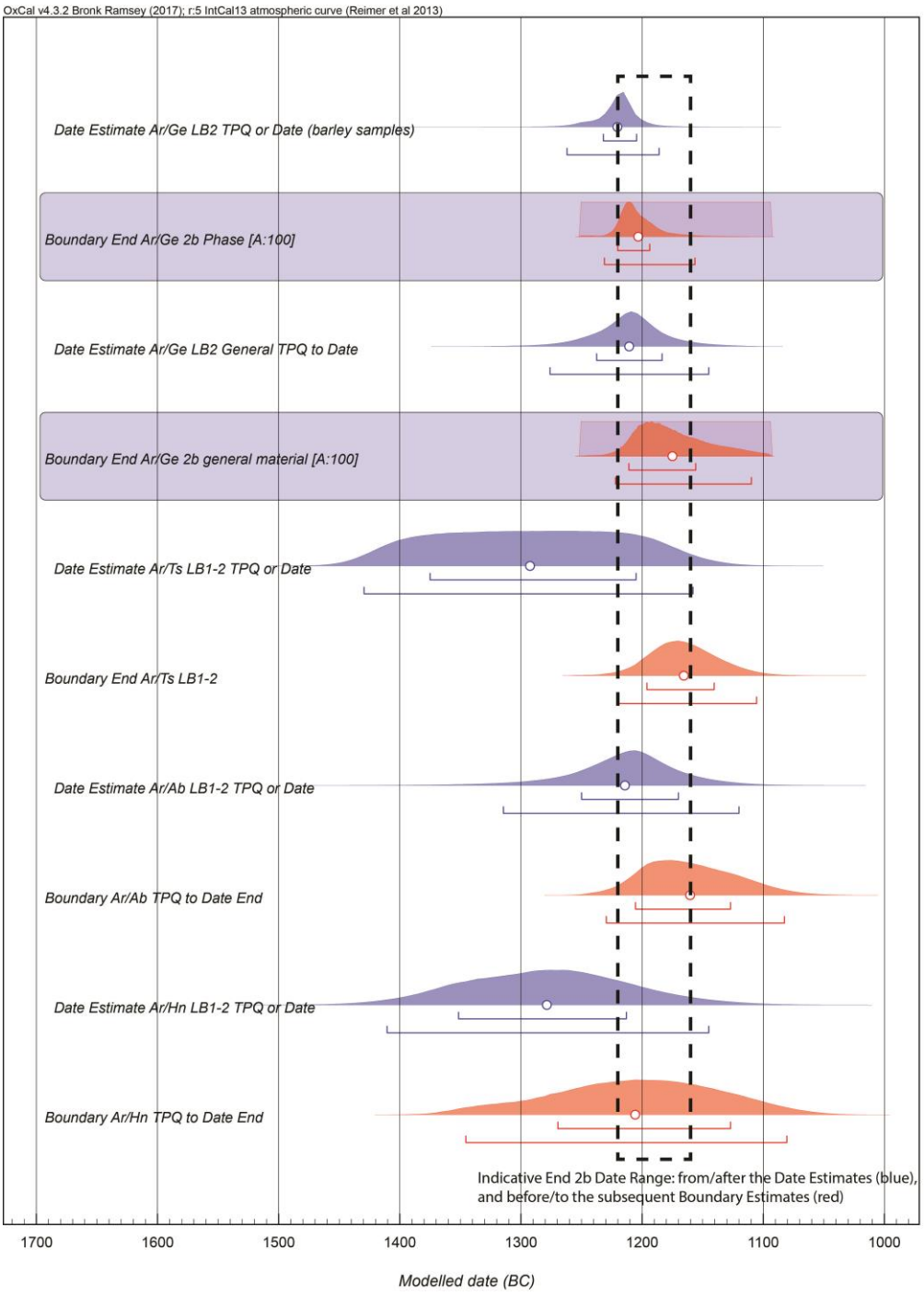

Figure S3. Selected elements from Figure S1 (see also Figure 3) for the modelled dates for the Late Bronze 2 (Stratum 2b, Stratum 2, or Stratum 1-2) contexts (date estimates as TPQ to date ranges) in blue and the subsequent Boundaries offering dates estimates as *terminus ante quem* to date ranges for the end/close of the Late Bronze 2 at each of the sites in red. The end of Late Bronze 2 destructions likely occurred somewhere in-between as indicated in approximate terms

by the dashed box, covering *c*. 1220–1160 BC The small circles under each probability distribution indicate the means (μ) of the distributions.

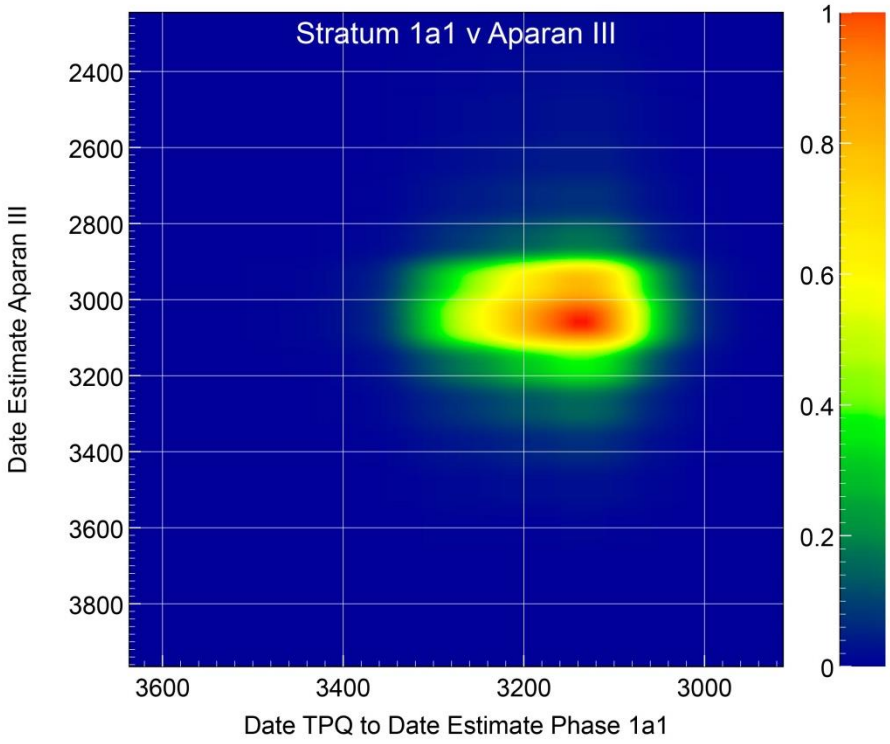

Figure S4. Correlation plot between modelled data from Gegharot stratum 1a1 versus Aparan III. While there is overlap, the Aparan III probability centres more ca. 3100-3000 BC, while the Gegharot stratum 1a1 probability centres more *c*. 3100–3200 BC

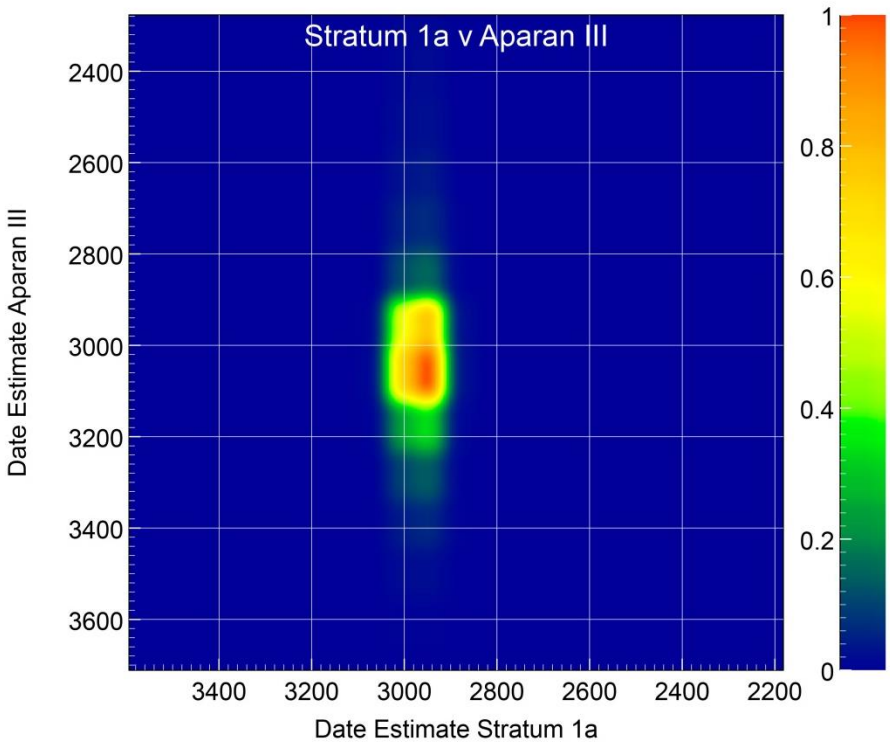

Figure S5. Correlation plot between modelled data from Gegharot stratum 1a versus Aparan III. While there is again overlap, the Aparan III probability centres more ca. 3100-3000 BC, while the Gegharot stratum 1a probability centres more *c*. 3000–2900 BC

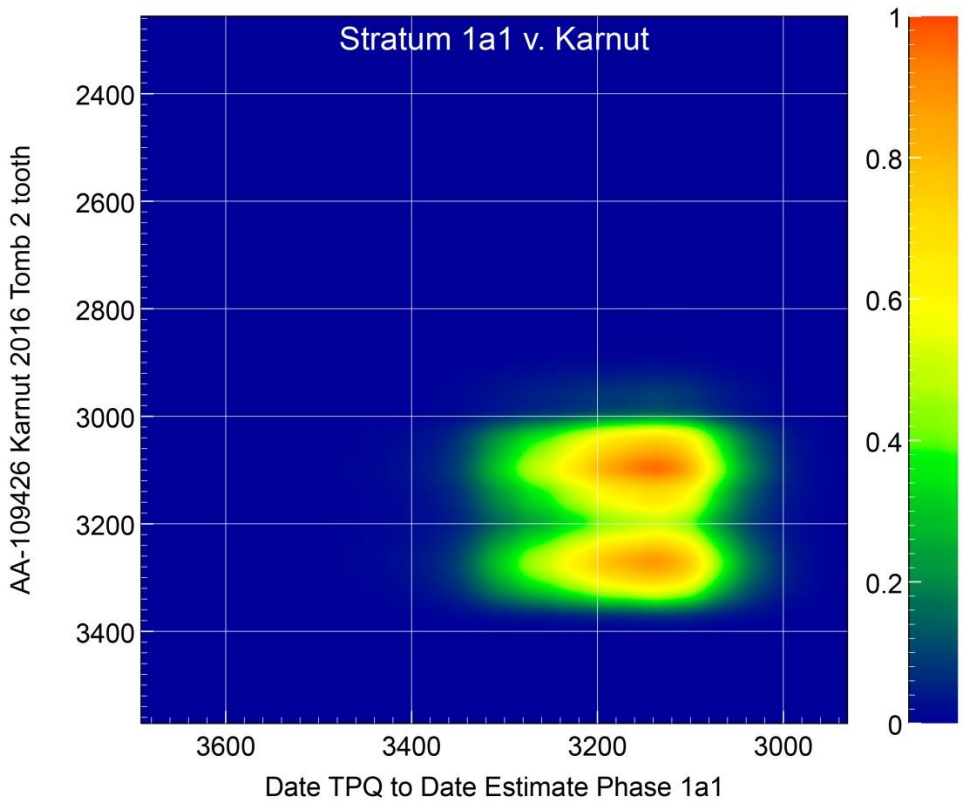

Figure S6. Correlation plot between modelled data from Gegharot stratum 1a1 versus a date on a tooth from a Karnut tomb. There is reasonable overlap in the range *c*. 3200–3100 BC but the Karnut date includes also an earlier range *c*. 3300–3200 BC It is important to note that the Karnut evidence comes from a single date at this stage.

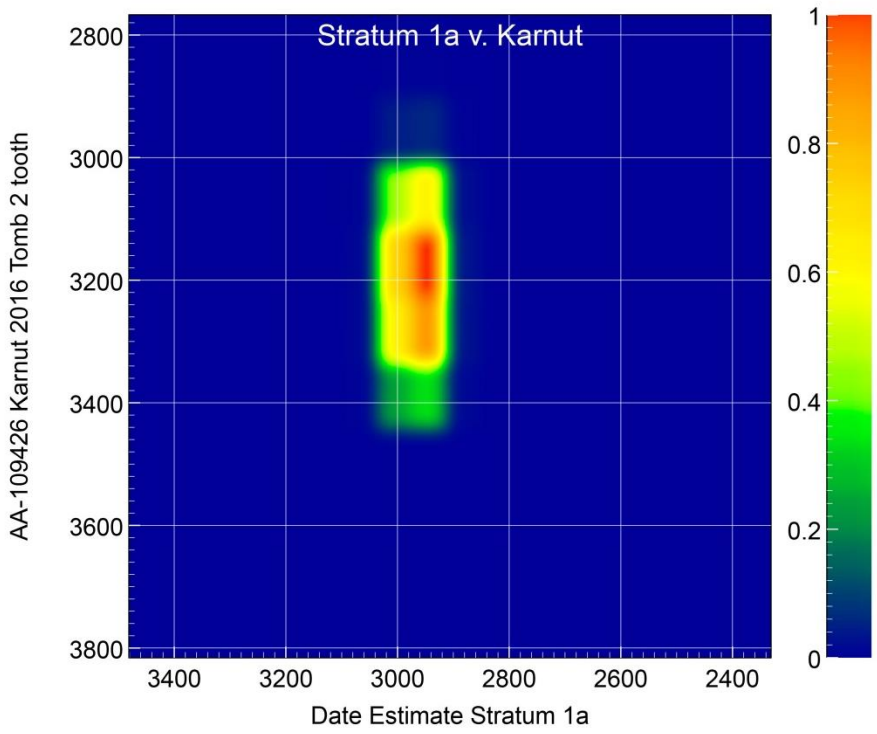

Figure S7. Correlation plot between modelled data from Gegharot stratum 1a versus a date on a tooth from a Karnut tomb. There is little overlap. The Gegharot 1a probability centres 3000–2900 BC, whereas the Karnut probability centres *c*. 3100–3300 BC. It is important to note that the Karnut evidence comes from a single date at this stage.

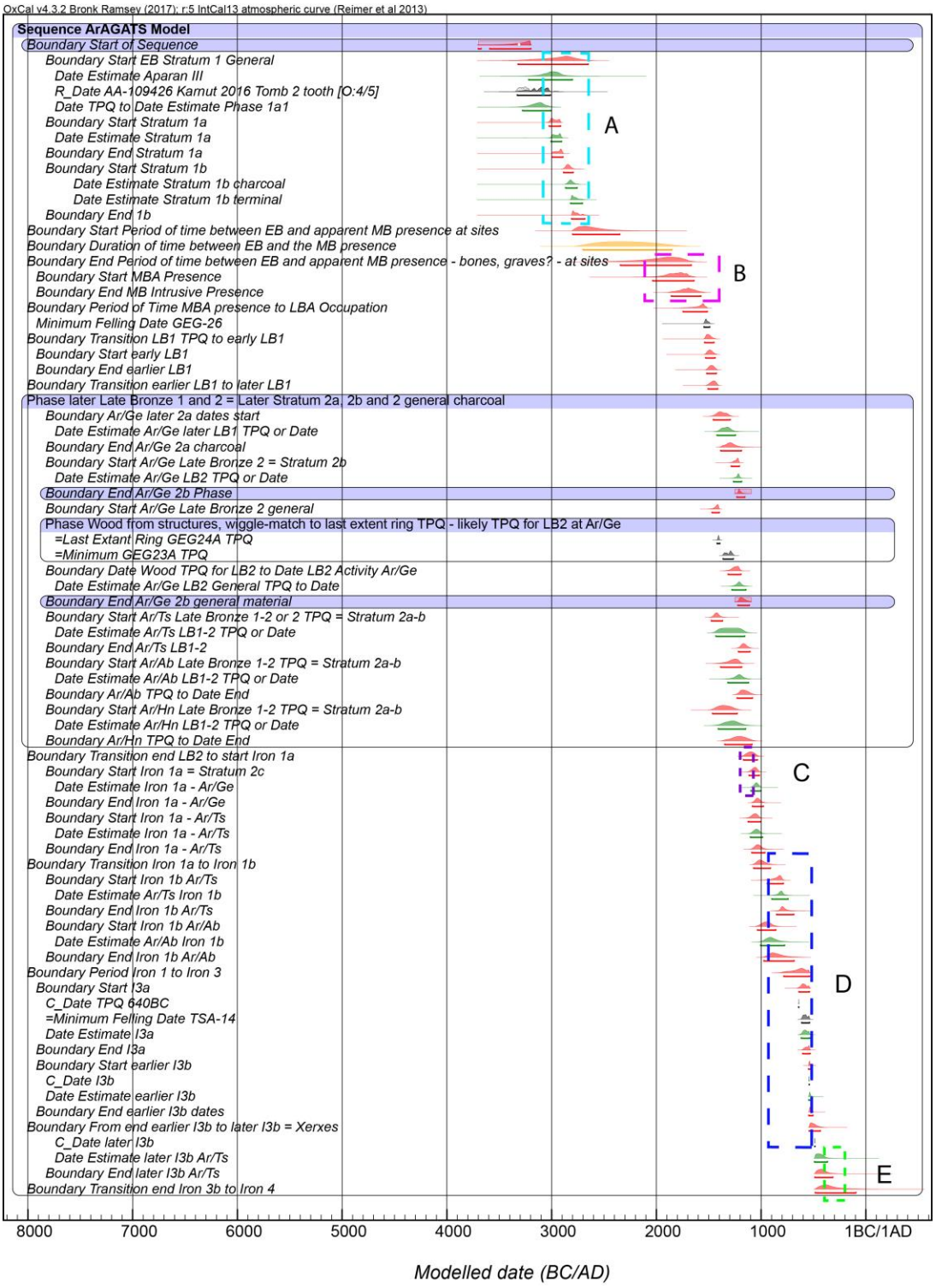

Figure S8. Summary of the main elements in Model 3 (Figure S1, Table S2) shown against: A. the 68.2 per cent probability overall Kura-Araxes II ('Interval') range from Passerini *et al*. 2016; B. the Middle Bronze Age range in Cherry *et al*. (2007); C. the early Iron Age range in Cherry *et*

al. (2007); D. the later Iron Age range in Cherry *et al*. (2007); and E. the later Achaemenid/Yervandid range in Cherry *et al*. (2007).

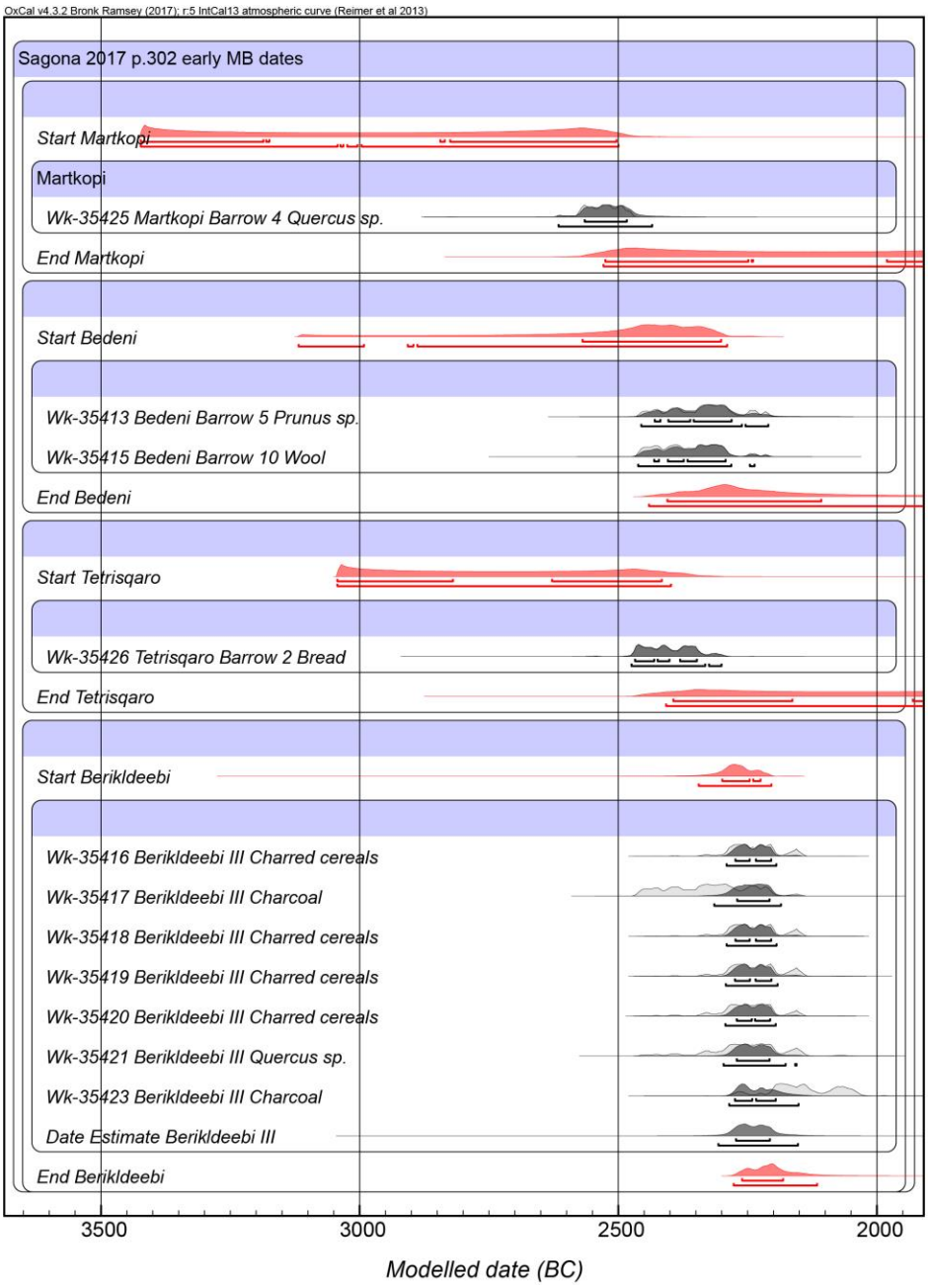

Figure S9. Radiocarbon dates from early MBA contexts from Sagona (2017: 302) modelled as separate site Sequences and Phases within an overall Early MB Phase (using Bronk Ramsey 2009a; 2009b Reimer *et al*. 2013). As in the ArAGATS Model 3 (see above), the Charcoal Plus Outlier model is applied to the dates on charcoal (to take some account of the effect of in-built age) and the General Outlier model is applied to the dates on short-lived samples. The Martkopi date is identified as Wk-35425 from the plot in the lower portion of Sagona (2017: Fig.7.2), whereas there are two dates labelled as Wk-35426 in the upper part of the figure. Sagona (2017:

302) reports the (non-modelled) 95.4 per cent calendar date range for Wk-35425 from Martkopi Barrow 4 as 2587–2474 BC. The start of the range is incorrect and is in fact the start of the 68.2 per cent probability range. The non-modelled 95.4 per cent range is 2617–2472 BC (our modelled range in Figure S9 is 2566–2484 at 68.2 per cent probability and 2616–2435 BC at 95.4 per cent probability).

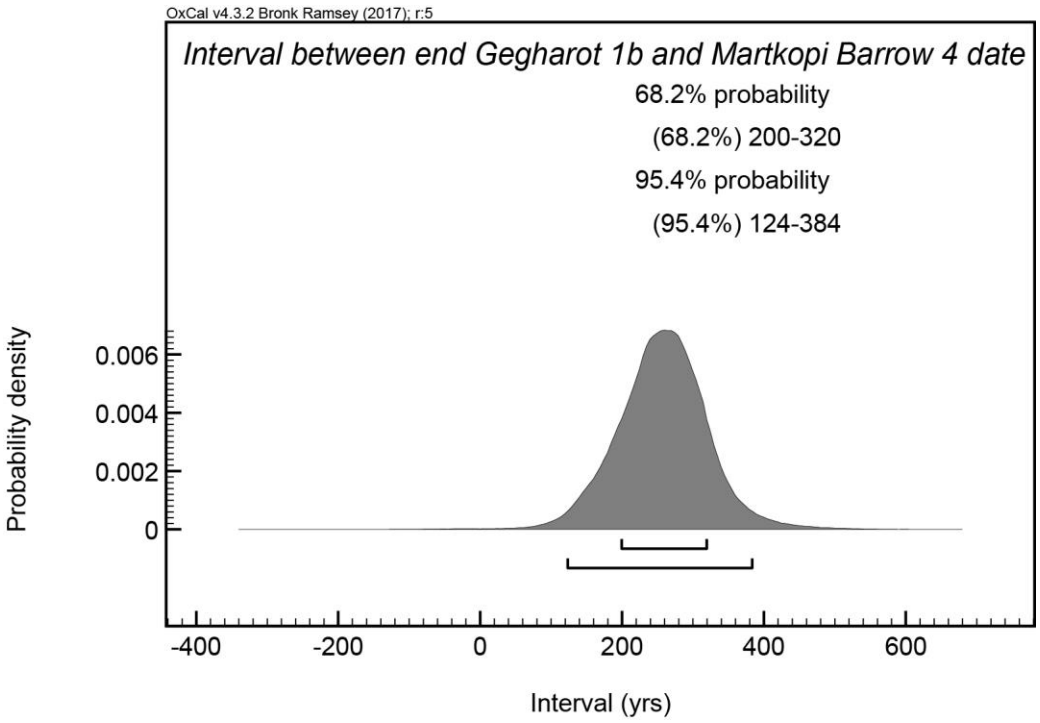

Figure S10. The interval (span of time) in calendar years between the end of Gegharot 1b as shown in Model 3 and the Wk-35425 date for Martkopi Barrow 4 as shown in Figure S9.

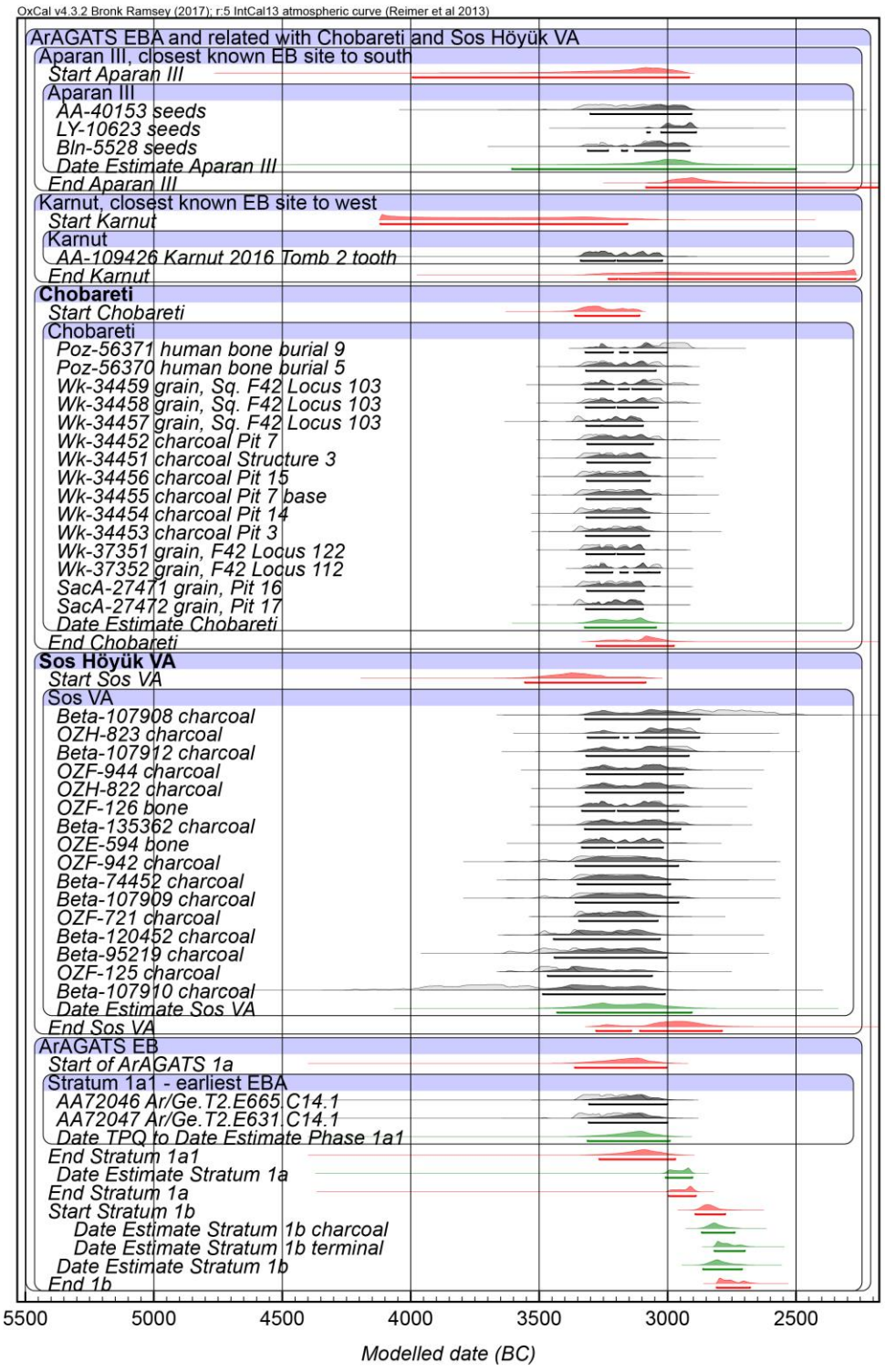

Figure S11. The dates for the early EBA contexts from Project ArAGATS and Aparan III and Karnut (as in Figure S1) compared with the dates from Chobareti in southern Georgia and Sos Höyük VA in eastern Turkey (bold labels) (Sagona 2014; Kakhiani *et al*. 2013 – see OSM text) – Chobareti and Sos Höyük considered as independent (overlapping) Sequences and Phases – with

modelling otherwise as in Model 3 (see above). Only the 95.4 per cent probability ranges are indicated under each probability distribution for clarity.

Table S1. OxCal Runfile (Model 3) for the ArAGATS data employed.

// indicates comments, and/or data excluded as outliers or context problems – see comments and see SI Text for discussion and explanations.

For the Prior file required to run the Charcoal Plus Outlier model, see Table S3 below.

An alternative section of code relating to Ar/Ge Stratum 2a and Stratum 2b – see SI Text – is listed at the end; its placement in the main runfile for an alternative model run (Model 3a) is noted by yellow highlighted comments (//) – these yellow highlighted sections are not part of the OxCal runfile. For comparisons in results, see SI Text, Table S2 and Figure S1K.

```
Options()
 {
  kIterations=200;
 };
 Plot()
 {
  Outlier_Model("IA",Prior("Charcoal_Plus"),U(0,3),"t");
  Outlier_Model("General",T(5),U(0,4),"t");
  Outlier_Model("RScaled",T(5),U(0,4),"r");
  R_Combine ("Ar/Ge LB2 Destruction SL Weighted Av.")
  {
   R_Date ("MAMS12403 C-AR-GEG T27.11 A barley", 2996,21);
   R_Date ("MAMS12404 C-AR-GEG T27.11 B barley", 2985,21);
   R_Date ("AA104305A C-AR-GEG T27.11 C barley", 2964,19);
   R_Date ("AA104305B C-AR-GEG T27.11 C barley", 2969,19);
   //R_Date ("AA104305C C-AR-GEG T27.11 C barley", 3051,21);
   R_Date ("AA104305D C-AR-GEG T27.11 C barley", 2980,21);
```

```
};
Sequence ("Ar/Ge LB2 Destruction SL Tau_Boundary Model")
{
 Tau_Boundary ("T")
 {
  color="Red";
 };
 Phase ()
 {
  R_Date ("MAMS12403 C-AR-GEG T27.11 A barley", 2996,21)
  {
   Outlier("General",0.05);
  };
  R_Date ("MAMS12404 C-AR-GEG T27.11 B barley", 2985,21)
  {
   Outlier("General",0.05);
  };
  R_Date ("AA104305A C-AR-GEG T27.11 C barley", 2964,19)
  {
   Outlier("General",0.05);
  };
  R_Date ("AA104305B C-AR-GEG T27.11 C barley", 2969,19)
  {
   Outlier("General",0.05);
  };
  //R_Date ("AA104305C C-AR-GEG T27.11 C barley", 3051,21)
  //{
  //     Outlier("General",0.05);
  //};
  R_Date ("AA104305D C-AR-GEG T27.11 C barley", 2980,21)
  {
```

```
  Outlier("General",0.05);
 };
};
Boundary ("Ar/Ge LB2 Destruction Tau_Boundary")
{
 color="Red";
};
};
D_Sequence ("C-AR-GEG-23A, Betula sp., W. side citadel 2a or 2b?")
{
R_Date ("MAMS12408rev RY1001-1010", 3074,25)
{
 Outlier("RScaled",0.05);
};
Gap(20);
//R_Date ("MAMS12409rev RY1011-1020", 2962,25)
//{
// Outlier("RScaled",0.05);
//};
//Gap(10); LARGE OUTLIER CUT
R_Date ("MAMS12410rev RY1021-1030", 3094,25)
{
 Outlier("RScaled",0.05);
};
Gap(10);
R_Date ("MAMS12411rev RY1031-1040", 3057,24)
{
 Outlier("RScaled",0.05);
};
Gap(10);
R_Date ("MAMS12412rev RY1041-1050", 3071,28)
```

```
 {
  Outlier("RScaled",0.05);
 };
 Gap(11.5);
 Date ("Minimum GEG23A TPQ");
 //57 extant rings no sapwood or bark evident
};
D_Sequence( "GEG24A, Pinus sp. Hd")
{
 First( );
 R_Date ("Hd-29849 C-AR-GEG-24A RY 1001 1010 = 1005.5", 3198, 12)
 {
  Outlier("RScaled",0.05);
 };
 Gap (0.5);
 //R_Date ("MAMS-12413 C-AR-GEG-24A Rings 1001 1010 = 1005.5", 3097, 27)
 //{
 // Outlier("RScaled",0.05);
 //};
 R_Date ("AA101105 Ar/Ge.T27.29 GEG-24A RY1001-1011 = 1006",3214,35)
 {
  Outlier("RScaled",0.05);
 };
 Gap (9.5);
 R_Date ("Hd-29850 C-AR-GEG-24A RY 1011 1020 A Set = 1015.5", 3165, 15)
 {
  Outlier("RScaled",0.05);
 };
 Gap (10);
 //R_Date ("MAMS-12414 C-AR-GEG-24A Rings 1011 1020 A Set = 1015.5", 3063, 23)
 //{
```

```
 // Outlier("RScaled",0.05);
 //};
 R_Date ("Hd-29852 C-AR-GEG-24A RY 1021 1030 A Set = 1025.5", 3129, 14)
 {
  Outlier("RScaled",0.05);
 };
 Gap (10);
 //R_Date ("MAMS-12415 C-AR-GEG-24A Rings 1021 1030 A Set = 1025.5", 3085, 23)
 //{
 // Outlier("RScaled",0.05);
 //};
 R_Date ("Hd-29851 C-AR-GEG-24A RY 1031 1040 = 1035.5", 3162, 15)
 {
  Outlier("RScaled",0.05);
 };
 Gap(10.5);
 Date ("Last Extant Ring GEG24A TPQ");
 //46 extant rings, NO bark or outermost ring
};
//Note issues GEG23A and 24A with original MAMS date runs - revised dates from 2nd run for
GEG23A; hence prefer and use Hd and as supported by AA values for GEG24A
Page();
Sequence ("TSA-14")
{
 D_Sequence ("TSA-14, Quercus sp.")
 {
  First ();
  R_Date ("AA101680 Rings 1001-1005", 2478, 21)
  {
   Outlier("RScaled",0.05);
  };
```

```
Gap (5);
R_Date ("AA101681 Rings 1006-1010", 2485, 28)
{
 Outlier("RScaled",0.05);
};
Gap (5);
R_Date ("AA101682 Rings 1011-1015", 2467, 24)
{
 Outlier("RScaled",0.05);
};
Gap (5);
R_Date ("AA101683 Rings 1016-1020", 2496, 22)
{
 Outlier("RScaled",0.05);
};
Gap (5);
R_Date ("AA101684 Rings 1021-1025", 2507, 19)
{
 Outlier("RScaled",0.05);
};
Gap (5);
R_Date ("AA101685 Rings 1026-1030", 2503, 25)
{
 Outlier("RScaled",0.05);
};
Gap (5);
R_Date ("AA101686 Rings 1031-1035", 2490, 19)
{
 Outlier("RScaled",0.05);
};
Gap(4);
```

```
 Date ("Last Extant Ring TSA-14 - no sapwood");
 };
 Label ("Estimated Minimum Bark Date with 15 +/- 5 sapwood rings as estimate for younger
Quercus");
 Interval("Gap Until Estimated Bark 2", N(15, 5));
 Date("Minimum Felling Date TSA-14");
};
Page();
Sequence ("ArAGATS Model")
{
 Boundary( "Start of Sequence", Date(U(-3700,-3200)))
 {
  color="Red";
 };
 Phase ("ArAGATS EBA and related")
 {
  //NOTE for EBA Sequence all samples wood charcoal UNLESS noted
  Sequence ()
  {
   Boundary ("Start EB Stratum 1 General")
   {
    color="Red";
   };
   Phase ("General EB - Stratum 1 samples including other ArAGATS sites")
   {
    R_Date ("AA92840 Ar/Ts.WSAD.31.C14.01", 4370,180)
    {
     Outlier("IA", 1);
    };
    R_Date ("AA105116 Ar/Ab.AB4.29.C14.01", 4132, 46)
    {
```

```
  Outlier("IA", 1);
 };
};
Boundary ("End EB - Stratum 1 General")
{
 color="Red";
};
};
Sequence ("Aparan III, closest known EB site to south")
{
Boundary ("Start Aparan III")
{
 color="Red";
};
Phase ("Aparan III")
{
 R_Date ("AA-40153 seeds",4455,75)
 {
  Outlier ("General",0.05);
 };
 R_Date ("LY-10623 seeds",4321,33)
 {
  Outlier ("General",0.05);
 };
 R_Date ("Bln-5528 seeds",4428,39)
 {
  Outlier ("General",0.05);
 };
 Date("Date Estimate Aparan III")
 {
  color="Green";
```

```
  };
 };
 Boundary ("End Aparan III")
 {
  color="Red";
 };
};
Sequence ("Karnut, closest known EB site to west")
{
 Boundary ("Start Karnut")
 {
  color="Red";
 };
 Phase ("Karnut")
 {
  R_Date ("AA-109426 Karnut 2016 Tomb 2 tooth",4463,32)
  {
   Outlier ("General",0.05);
  };
 };
 Boundary ("End Karnut")
 {
  color="Red";
 };
};
Sequence("ArAGATS EB")
{
 Boundary( "Start of ArAGATS 1a")
 {
  color="Red";
 };
```

```
Phase ("Stratum 1a1 - earliest EBA")
{
 R_Date("AA72046 Ar/Ge.T2.E665.C14.1",4492,41)
 {
  Outlier("IA", 1);
 };
 R_Date("AA72047 Ar/Ge.T2.E631.C14.1",4523,49)
 {
  Outlier("IA", 1);
 };
 Date("Date TPQ to Date Estimate Phase 1a1")
 {
  color="Green";
 };
};
Boundary ("End Stratum 1a1")
{
 color="Red";
};
Boundary ("Interval between 1a1 and 1a?")
{
 color="Orange";
};
Boundary ("Start Stratum 1a")
{
 color="Red";
};
Phase ("1a/EB1")
{
 R_Date ("AA52898 Ar/Ge.T10a.3.C14.1 bone",4314,60)
 {
```

```
 Outlier ("General",0.05);
};
//sample bone in spreadsheet under EB and stratum 1 and "lower", so let us assume likely 1a
R_Date("AA72060 Ar/Ge.T17.104.C14.1",4346,38)
{
 Outlier("IA", 1);
};
R_Date("AA72070 Ar/Ge.T18.32.C14.1",4389,37)
{
 Outlier("IA", 1);
};
R_Date ("AA95616 Ar/Ge.T28.41.C14.02", 4374,42)
{
 Outlier("IA", 1);
};
R_Date("AA56969 Ar/Ge.T12.2.C14.1",4285,43)
{
 Outlier("IA", 1);
};
R_Date ("AA105121 Ar/Ge.T30.88.C14.02",4389,28)
{
 Outlier("IA", 1);
};
R_Date ("AA105128 Ar/Ge.T30.28.C14.03",4397,37)
{
 Outlier("IA", 1);
};
R_Date ("AA105129 Ar/Ge.T30.96.C14.02",4363,33)
{
 Outlier("IA", 1);
};
```

```
R_Date ("AA105130 Ar/Ge.T30.81.C14.04",4416,33)
{
 Outlier("IA", 1);
};
R_Date ("AA102808 Ar/Ge.T30.65.C14.03",4359,51)
{
 Outlier("IA", 1);
};
R_Date ("AA109433 Ar/Ge.T38.41.C14.01", 4459,23)
{
 Outlier("IA", 1);
};
R_Date ("AA109432 Ar/Ge.T38.07.C14.03", 4340,22)
{
 Outlier("IA", 1);
};
R_Date("AA72213 Ar/Ge.T2.E669.C14.1 bone",4293,44)
{
 Outlier ("General",0.05);
};
R_Date("AA72214 Ar/Ge.T2.E670.C14.1 bone",4286,42)
{
 Outlier ("General",0.05);
};
R_Date("AA72061 Ar/Ge.T17.104.C14.2 seeds",4371,38)
{
 Outlier ("General",0.05);
};
R_Date("AA72069 Ar/Ge.T18.26.C14.1 seeds",4402,38)
{
 Outlier ("General",0.05);
```

```
};
R_Date ("AA102806 Ar/Ge.T30.67.C14.01 seeds",4337,43)
{
 Outlier ("General",0.05);
};
Date ("Date Estimate Stratum 1a")
{
 color="Green";
};
Span("Duration Stratum 1a");
};
Boundary ("End Stratum 1a")
{
 color="Red";
};
Boundary ("Start 1a-1b transition phase")
{
 color="Red";
};
Phase ("TPQ to Date for Time Period Between main 1a and main 1b, or after AA102808 and
102806")
{
 R_Date ("AA95618 Ar/Ge.T28.34.C14.01", 4391, 49)
 {
  Outlier("IA", 1);
 };
 //stated after AA102808 and 102806
 R_Date ("AA102809 Ar/Ge.T30.63.C14.01",4389,43)
 {
  Outlier("IA", 1);
 };
```

```
//stated must be later than AA102808 & 102806, so 1a or later - but age 1a and NOT 1b, so assume also in the 1a-1b transition period
R_Date ("AA109435 Ar/Ge.T38.32.C14.02", 4267,22)
{
 Outlier("IA", 1);
};
R_Date ("AA109436 Ar/Ge.T38.32.C14.01", 4372,25)
{
 Outlier("IA", 1);
};
//could be later than AA109433 as evidence of re-flooring over the hearth
Date("Date TPQ to Date Estimate Time Period Between 1a and 1b")
{
 color="Green";
};
};
Boundary ("End 1a-1b transition period")
{
 color="Red";
};
Boundary ("Start Stratum 1b")
{
 color="Red";
};
Phase ("1b overall")
{
 Sequence ()
 {
  Phase ("1b/EB2 charcoal")
  {
   R_Date("AA72066 Ar/Ge.T18.13.C14.1",4201,37)
```

```
{
 Outlier("IA", 1);
};
R_Date("AA72045 Ar/Ge.T2.E659.C14.2",4077,41)
{
 Outlier("IA", 1);
};
R_Date("AA52900 Ar/Ge.T02c.10.C14.1",4197,40)
{
 Outlier("IA", 1);
};
R_Date("AA56968 Ar/Ge.T02d/e.6.C14.1",4105,41)
{
 Outlier("IA", 1);
};
R_Date("AA66894 Ar/Ge.T2.E565.C14.2",4130,45)
{
 Outlier("IA", 1);
};
R_Date("AA66895 Ar/Ge.T2.E565.C14.1",4104,47)
{
 Outlier("IA", 1);
};
R_Date ("AA92621 Ar/Ge.T28.21.C14.01", 4104,40)
{
 Outlier("IA", 1);
};
R_Date ("AA95617 Ar/Ge.T28.38.C14.02", 4119,42)
{
 Outlier("IA", 1);
};
```

```
 R_Date ("AA72053 Ar/Ge.T16.114.C14.1",4171,37)
 {
  Outlier("IA", 1);
 };
 R_Date ("AA92622 Ar/Ge.T22.105.C14.06", 4128,41)
 {
  Outlier("IA", 1);
 };
 R_Date ("AA92623 Ar/Ge.T20.104.C14.02", 4283,40)
 {
  Outlier("IA", 1);
 };
 R_Date ("AA92844 Ar/Ge.T19.112.C14.1", 4204, 52)
 {
  Outlier("IA", 1);
 };
 R_Date ("AA95615 Ar/Ge.T30.22.C14.01", 4104,40)
 {
  Outlier("IA", 1);
 };
 R_Date ("AA102807 Ar/Ge.T30.66.C14.01",4434,43)
 {
  Outlier("IA", 1);
 };
 Date ("Date Estimate Stratum 1b charcoal")
 {
  color="Green";
 };
};
Boundary ("Interval 1b general to 1b terminal")
{
```

```
 color="Red";
};
Phase ("1b Terminal")
{
 Sequence ("Terminal 1b teeth sequence")
 {
  Phase ("earlier to no later than next")
  {
   R_Date("AA109430 Ar/Ge T38.43.C14.02 tooth",4174,28)
   {
    Outlier ("General",0.05);
   };
   R_Date("AA109431 Ar/Ge T38.44.C14.01 tooth",4144,28)
   {
    Outlier ("General",0.05);
   };
  };
  Phase ("later or same age as previous")
  {
   R_Date("AA109427 Ar/Ge T38.18.C14.01 tooth",4156,31)
   {
    Outlier ("General",0.05);
   };
   R_Date("AA109428 Ar/Ge T38.18.C14.02 tooth",4169,28)
   {
    Outlier ("General",0.05);
   };
   R_Date("AA109429 Ar/Ge T38.18.C14.03 tooth",4247,28)
   {
    Outlier ("General",0.05);
   };
```

```
      };
     };
     R_Date("AA72067 Ar/Ge.T18.13.C14.2 seeds",4080,38)
     {
      Outlier ("General",0.05);
     };
     Date ("Date Estimate Stratum 1b terminal")
     {
      color="Green";
     };
    };
   };
   Date ("Date Estimate Stratum 1b")
   {
    color="Green";
   };
   Interval("Duration Stratum 1b");
  };
  Boundary("End 1b")
  {
   color="Red";
  };
 };
};
Boundary ("Start Period of time between EB and apparent MB presence at sites")
{
 color="Red";
};
Boundary("Duration of time between EB and the MB presence")
{
 color="Orange";
```

```
  };
  Boundary ("End Period of time between EB and apparent MB presence - bones, graves? - at
sites")
  {
   color="Red";
  };
  Sequence ()
  {
   Boundary ("Start MBA Presence")
   {
    color="Red";
   };
   Phase ("MBA Presence")
   {
    R_Date("AA52899 Ar/Ge.T10a.3.C14.2 bone stratum 1",3441,51);
    R_Date("AA56976 Ar/Ts.C6.7.C14.1 bone stratum 3",3508,98);
    Interval ("Duration MBA Presence");
   };
   Boundary ("End MB Intrusive Presence")
   {
    color="Red";
   };
  };
  Boundary ("Period of Time MBA presence to LBA Occupation")
  {
   color="Red";
  };
  Sequence ("GEG-26A - likely start/early LBA TPQ from LBA midden")
  {
   D_Sequence ("GEG-26A, Quercus sp.")
   {
```

```
First ();
R_Date ("AA101110 RY1001-1010", 3409, 36)
{
 Outlier("RScaled",0.05);
};
Gap (20);
R_Date ("AA101111 RY1020-1029", 3421, 30)
{
 Outlier("RScaled",0.05);
};
Gap (20);
R_Date ("AA101112 RY1040-1049", 3333, 29)
{
 Outlier("RScaled",0.05);
};
Gap(20);
R_Date ("AA101113 RY1060-1069", 3363, 36)
{
 Outlier("RScaled",0.05);
};
Gap(20);
R_Date ("AA101114 RY1080-1089", 3354, 38)
{
 Outlier("RScaled",0.05);
};
Gap(20);
R_Date ("AA101115 RY1100-1109", 3295, 47)
{
 Outlier("RScaled",0.05);
};
Gap(19.5);
```

```
     R_Date ("AA101116 RY1120-1128", 3343, 39)
     {
      Outlier("RScaled",0.05);
     };
     Gap (20);
     R_Date ("AA101117 RY1139-1148", 3252, 36)
     {
      Outlier("RScaled",0.05);
     };
     Gap(18.5);
     R_Date ("AA101118 RY1159-1165", 3349, 42)
     {
      Outlier("RScaled",0.05);
     };
     Gap (18);
     Date ("Last Preserved Tree-Ring RY1180");
    };
    Label ("Estimated Minimum Bark Date with 20 +/- 5 sapwood rings as 180+ years old
Quercus");
    Interval("Gap Until Estimated Bark 1", N(20, 5));
    Date("Minimum Felling Date GEG-26");
   };
   Boundary ("Transition LB1 TPQ to early LB1")
   {
    color="Red";
   };
   Sequence ()
   {
    Boundary ("Start early LB1")
    {
     color="Red";
```

```
};
Phase ("Ar/Ge early Late Bronze 1 = early Kurgan")
{
 R_Date("AA102805 Ar/Ge.K2.8.C14.01 charcoal 2a early",3320,110)
 {
  Outlier("IA", 1);
 };
 Date ("Date Estimate Ar/Ge earlier LB1 TPQ or Date")
 {
  color="Green";
 };
};
Boundary ("End earlier LB1")
{
 color="Red";
};
};
Boundary ("Transition earlier LB1 to later LB1")
{
 color="Red";
};
Phase ("later Late Bronze 1 and 2 = Later Stratum 2a, 2b and 2 general charcoal")
{
 //Alternative Code Start – see below
 Sequence ("Ar/Ge 2a")
 {
  Boundary("Ar/Ge later 2a dates start")
  {
   color="Red";
  };
  Phase ("Ar/Ge 2a")
```

```
{
 R_Date("AA40149 Ar/Ge.T02.23.C14.01 charcoal 2a",3098,42)
 {
  Outlier("IA", 1);
 };
 R_Date("AA40151 Ar/Ge.T02.18.C14.01 charcoal 2a",3151,50)
 {
  Outlier("IA", 1);
 };
 R_Date("AA72048 Ar/Ge.T2.E645.C14.1 charcoal 2a",3017,41)
 {
  Outlier("IA", 1);
 };
 R_Date("AA72049 Ar/Ge.T2.E626.C14.2 charcoal 2a",3117,41)
 {
  Outlier("IA", 1);
 };
 R_Date("AA95613 Ar/Ge.T31.41.C14.01 charcoal 2a?",3094,39)
 {
  Outlier("IA", 1);
 };
 R_Date("AA105124 Ar/Ge.K3.28.C14.03 charcoal 2a",3069,39)
 {
  Outlier("IA", 1);
 };
 R_Date("AA105137 Ar/Ge.K3.28.C14.01 charcoal 2a",3223,67)
 {
  Outlier("IA", 1);
 };
 R_Date("AA105138 Ar/Ge.K3.28.C14.02 charcoal 2a",3098,47)
 {
```

```
  Outlier("IA", 1);
 };
 Date ("Date Estimate Ar/Ge later LB1 TPQ or Date")
 {
  color="Green";
 };
 Interval ("Duration Ar/Ge later LB1");
};
Boundary ("End Ar/Ge 2a charcoal")
{
 color="Red";
};
};
Sequence (“Ar/Ge 2b”)
{
Boundary ("Start Ar/Ge Late Bronze 2 = Stratum 2b")
{
 color="Red";
};
Phase ("Ar/Ge 2b")
{
 R_Date("AA52901 Ar/Ge.T02c.19.C14.1 charcoal 2b",2961,37)
 {
  Outlier("IA", 1);
 };
 //AA52901 - hard to push to Iron 1 based on stratigraphy so leave as LBA
 R_Date("AA56970 Ar/Ge.T2E.208.C14.3 charcoal 2b",3020,35)
 {
  Outlier("IA", 1);
 };
 R_Date("AA66886 Ar/Ge.T15.B3.C14.1 charcoal 2b",3081,37)
```

```
{
 Outlier("IA", 1);
};
//R_Date("AA66888 Ar/Ge.T15.C14.C14.1 charcoal 2b",4313,39)
//{
// Outlier("IA", 1);
//};
//Outlier INITIAL CUT AS RESIDUAL
R_Date("AA66890 Ar/Ge.T15.C25.C14.1 charcoal2b",2988,37)
{
 Outlier("IA", 1);
};
R_Date("AA66896 Ar/Ge.T2.E522.C14.1 charcoal 2b",3082,35)
{
 Outlier("IA", 1);
};
R_Date("AA66898 Ar/Ge.T2.E513.C14.1 charcoal 2b",3001,40)
{
 Outlier("IA", 1);
};
R_Date("AA92625 Ar/Ge.T21.06.C14.02 charcoal 2b",2971,39)
{
 Outlier("IA", 1);
};
R_Date("AA95614 Ar/Ge.T31.07.C14.01 charcoal 2b?",3039,40)
{
 Outlier("IA", 1);
};
Label ("T27 - 2b?");
R_Date ("MAMS12406 C-AR-GEG T27 12A poplar",3033,25)
{
```

```
 Outlier("IA", 1);
};
R_Date ("MAMS12407A C-AR-GEG T27 5A wood charcoal",2990,31)
{
 Outlier("IA", 1);
};
R_Date ("MAMS12407B C-AR-GEG T27 5A",3032,26)
{
 Outlier("IA", 1);
};
R_Date("AA102811 Ar/Ge.T30.50.C14.01 charcoal 2b?",3049,41)
{
 Outlier("IA", 1);
};
R_Date("AA106847 Ar/Ge.T30.108.C14.01 charcoal 2 = 2b?",3019,27)
{
 Outlier("IA", 1);
};
R_Date ("MAMS12403 C-AR-GEG T27.11 A barley A", 2996,21)
{
 Outlier ("General",0.05);
};
R_Date ("MAMS12404 C-AR-GEG T27.11 B barley B", 2985,21)
{
 Outlier ("General",0.05);
};
R_Date ("AA104305A C-AR-GEG T27.11 C barley C", 2964,19)
{
 Outlier ("General",0.05);
};
R_Date ("AA104305B C-AR-GEG T27.11 C barley D", 2969,19)
```

```
 {
  Outlier ("General",0.05);
 };
 //R_Date ("AA104305C C-AR-GEG T27.11 C barley E", 3051,21)
 //{
 // Outlier ("General",0.05);
 //};
 R_Date ("AA104305D C-AR-GEG T27.11 C barley F", 2980,21)
 {
  Outlier ("General",0.05);
 };
 Date ("Date Estimate Ar/Ge LB2 TPQ or Date")
 {
  color="Green";
 };
 Interval ("Duration Ar/Ge LB2");
};
Boundary ("End Ar/Ge 2b Phase",Date(U(-1251,-1093)))
{
 color="Red";
};
//95.4% range for End Tau Boundary Phase 5 SL 2b dates minus AA104305C
};
//Alternative Code End – see below
Sequence ()
{
 Boundary ("Start Ar/Ge Late Bronze 2 general")
 {
  color="Red";
 };
```

```
    Phase ("Wood from structures, wiggle-match to last extent ring TPQ - likely TPQ for LB2 at
Ar/Ge")
    {
     Date ("=Last Extant Ring GEG24A TPQ");
     Date ("=Minimum GEG23A TPQ");
    };
    Boundary ("Date Wood TPQ for LB2 to Date LB2 Activity Ar/Ge")
    {
     color="Red";
    };
    Phase ("Ar/Ge Stratum 2a-b general TPQ")
    {
     R_Date("AA40146 Ar/Ge.T01.04.C14.1 charcoal 2", 3035,41)
     {
      Outlier("IA", 1);
     };
     R_Date("AA40147 Ar/Ge.T01.07.C14.01 charcoal 2",3083,52)
     {
      Outlier("IA", 1);
     };
     R_Date("AA40150 Ar/Ge.T02.16.C14.01 charcoal 2",2982,42)
     {
      Outlier("IA", 1);
     };
     R_Date("AA56967 Ar/Ge.T2D/a.24.C14.1 charcoal 2",2973,38)
     {
      Outlier("IA", 1);
     };
     R_Date("AA56973 Ar/Ge.T2D/a.26.C14.1 charcoal 2",3012,43)
     {
      Outlier("IA", 1);
```

```
};
R_Date("AA66892 Ar/Ge.T16.A11.C14.1 charcoal 2",3166,43)
{
 Outlier("IA", 1);
};
R_Date("AA66893 Ar/Ge.T16.A7.C14.1 charcoal 2",2990,42)
{
 Outlier("IA", 1);
};
R_Date("AA72044 Ar/Ge.T19.5.C14.1 charcoal 2",2941,39)
{
 Outlier("IA", 1);
};
R_Date("AA72051 Ar/Ge.T16.113.C14.1 charcoal 2",3007,36)
{
 Outlier("IA", 1);
};
R_Date("AA72052 Ar/Ge.T16.113.C14.2 charcoal 2",3162,36)
{
 Outlier("IA", 1);
};
R_Date("AA72059 Ar/Ge.T17.106.C14.1 charcoal 2",3002,35)
{
 Outlier("IA", 1);
};
R_Date("AA72062 Ar/Ge.T18.2.C14.1 charcoal 2",2996,36)
{
 Outlier("IA", 1);
};
R_Date("AA72063 Ar/Ge.T18.3.C14.1 charcoal 2",2974,35)
{
```

```
 Outlier("IA", 1);
};
R_Date("AA72064 Ar/Ge.T18.10.C14.5 charcoal 2",2972,36)
{
 Outlier("IA", 1);
};
R_Date("AA72065 Ar/Ge.T18.11.C14.2 charcoal 2",2984,37)
{
 Outlier("IA", 1);
};
R_Date("AA72068 Ar/Ge.T18.25.C14.1 charcoal 2",3010,36)
{
 Outlier("IA", 1);
};
R_Date("AA92627 Ar/Ge.T21.12.C14.01 charcoal 2",2943,39)
{
 Outlier("IA", 1);
};
R_Date("AA95611 Ar/Ge.T32.54.C14.01 charcoal 2",2960,43)
{
 Outlier("IA", 1);
};
R_Date("AA95980 Ar/Ge.T32.20.C14.01 charcoal 2",3015,40)
{
 Outlier("IA", 1);
};
R_Date("AA105126 AR/Ge.K2.107.C14.01 tooth 1",2939,32)
{
 Outlier ("General",0.05);
};
Date ("Date Estimate Ar/Ge LB2 General TPQ to Date")
```

```
 {
  color="Green";
 };
};
Boundary ("End Ar/Ge 2b general material",Date(U(-1251,-1093)))
{
 color="Red";
};
};
Sequence ()
{
Boundary ("Start Ar/Ts Late Bronze 1-2 or 2 TPQ = Stratum 2a-b")
{
 color="Red";
};
Phase ("Ar/Ts")
{
 R_Date("AA56982 Ar/Ts.SLT1.46 charcoal 2",3012,35)
 {
  Outlier("IA", 1);
 };
 R_Date("AA56987 Ar/Ts.SLT1.60 charcoal 2",3102,41)
 {
  Outlier("IA", 1);
 };
 R_Date("AA56983 Ar/Ts.SLT1.64 charcoal 2",2981,34)
 {
  Outlier("IA", 1);
 };
 R_Date("AA56985 Ar/Ts.SLT2.10 charcoal 2",3008,35)
 {
```

```
 Outlier("IA", 1);
};
R_Date("AA56986 Ar/Ts.SLT3.13 charcoal 2",3058,35)
{
 Outlier("IA", 1);
};
R_Date("AA66873 Ar/Ts.SLT4.14.C14.1 charcoal 2",2972,35)
{
 Outlier("IA", 1);
};
R_Date("AA82785 Ar/Ts.SLT8.9.C14.1 charcoal 2", 2993, 44)
{
 Outlier("IA", 1);
};
R_Date("AA82787 Ar/Ts.SLT8.12.C14.1 charcoal 2", 2883, 66)
{
 Outlier("IA", 1);
};
R_Date("AA92630 Ar/Ts.SLT9.21.C14.1 charcoal 2",3080,39)
{
 Outlier("IA", 1);
};
R_Date("AA92631 Ar/Ts.SLT9.35.C14.1 charcoal 2",3067,38)
{
 Outlier("IA", 1);
};
R_Date("AA92633 Ar/Ts.SLT10.14.C14.5 charcoal 2",3111,39)
{
 Outlier("IA", 1);
};
R_Date("AA92634 Ar/Ts.SLT10.16.C14.1 charcoal 2",3102,39)
```

```
{
 Outlier("IA", 1);
};
R_Date("AA92635 Ar/Ts.SLT10.19.C14.1 charcoal 2",3110,38)
{
 Outlier("IA", 1);
};
R_Date("AA95623 Ar/Ts.SLT14.5.C14.6 charcoal 2",3080,51)
{
 Outlier("IA", 1);
};
R_Date("AA95624 Ar/Ts.SLT14.9.C14.3 charcoal 2",3182,41)
{
 Outlier("IA", 1);
};
R_Date("AA95625 Ar/Ts.SLT14.12.C14.4 charcoal 2",3117,40)
{
 Outlier("IA", 1);
};
R_Date("AA95626 Ar/Ts.SLT14.14.C14.6 charcoal 2",3148,40)
{
 Outlier("IA", 1);
};
R_Date("AA82786 Ar/Ts.SS1.6.C14.1 charcoal 2",3231,39)
{
 Outlier("IA", 1);
};
R_Date("AA31034 Ar/Ts.WT01.08.C14.1 charcoal 2",3015,45)
{
 Outlier("IA", 1);
};
```

```
R_Date("AA31035 Ar/Ts.WT01.06.C14.1 charcoal 2",3040,45)
{
 Outlier("IA", 1);
};
R_Date("AA31036 Ar/Ts.WT01.05.C14.3 charcoal 2",2975,50)
{
 Outlier("IA", 1);
};
R_Date("AA52902 Ar/Ts.WT2.9.C14.1 charcoal 2",3100,38)
{
 Outlier("IA", 1);
};
R_Date("AA52903 Ar/Ts.C3.A11.C14.1 charcoal 2",2973,37)
{
 Outlier("IA", 1);
};
R_Date("AA52905 Ar/Ts.C3.B7.C14.1 charcoal 2",3088,37)
{
 Outlier("IA", 1);
};
R_Date("AA52906 Ar/Ts.C5.14.C14.1 charcoal 2",2997,38)
{
 Outlier("IA", 1);
};
R_Date("AA56978 Ar/Ts.C7.19.C14.1 charcoal 2",3094,35)
{
 Outlier("IA", 1);
};
R_Date("AA56979 Ar/Ts.C8.6.C14.3 charcoal 2",2949,34)
{
 Outlier("IA", 1);
```

```
};
R_Date("AA56980 Ar/Ts.C10.12.C14.1 charcoal 2",3023,34)
{
 Outlier("IA", 1);
};
R_Date("AA56981 Ar/Ts.C11.5.C14.1 charcoal 2",3045,40)
{
 Outlier("IA", 1);
};
R_Date("AA66878 Ar/Ts.ST2.4.C14.1 charcoal 2",3138,37)
{
 Outlier("IA", 1);
};
R_Date("AA66879 Ar/Ts.ST2.11.C14.1 charcoal 2",3070,40)
{
 Outlier("IA", 1);
};
R_Date("AA66881 Ar/Ts.WSC2.13.C14.3 charcoal 2",3193,38)
{
 Outlier("IA", 1);
};
R_Date("AA66883 Ar/Ts.WSL.13.C14.1 charcoal 2",3134,37)
{
 Outlier("IA", 1);
};
R_Date("AA66884 Ar/Ts.WSL.7.C14.2 charcoal 2",3100,38)
{
 Outlier("IA", 1);
};
R_Date("AA66885 Ar/Ts.WSL.20.C14.1 charcoal 2",3269,47)
{
```

```
 Outlier("IA", 1);
};
R_Date("AA92846 Ar/Ts.WSAD.32.C14.01 charcoal 2",2920,36)
{
 Outlier("IA", 1);
};
R_Date("AA92843 Ar/Ts.WSAC.30.C14.02 charcoal 2",2949,48)
{
 Outlier("IA", 1);
};
R_Date("AA96534 Ar/Ts.WSN.65.C14.02 charcoal 2",3132,38)
{
 Outlier("IA", 1);
};
R_Date("AA92839 Ar/Ts.WSI2.20.C14.01 charcoal 2",3186,37)
{
 Outlier("IA", 1);
};
R_Date("AA106848 Ar/Ts.BC12.T01.20.C14 wood 2",3051,28)
{
 Outlier("IA", 1);
};
R_Date("AA52908 Ar/Ts.NT1.A5.C14.1 charcoal 2b",3028,38)
{
 Outlier("IA", 1);
};
R_Date("AA52909 Ar/Ts.NT1.B16.C14.1 charcoal 2b",3094,46)
{
 Outlier("IA", 1);
};
R_Date("AA95622 Ar/Ts.SLT13.22.C14.1 charred pea 2",3185,87)
```

```
 {
  Outlier("General",0.05);
 };
 Date ("Date Estimate Ar/Ts LB1-2 TPQ or Date")
 {
  color="Green";
 };
};
Boundary ("End Ar/Ts LB1-2")
{
 color="Red";
};
};
Sequence ()
{
Boundary ("Start Ar/Ab Late Bronze 1-2 TPQ = Stratum 2a-b")
{
 color="Red";
};
Phase ("Ar/Ab")
{
 R_Date("AA82791 Ar/Ab.AB2.13.C14.02 charcoal 2",3078,35)
 {
  Outlier("IA", 1);
 };
 R_Date("AA82792 Ar/Ab.AB3.12.C14.01 charcoal 2",3040,35)
 {
  Outlier("IA", 1);
 };
 R_Date("AA82793 Ar/Ab.AB3.16.C14.01 charcoal 2",3005,36)
 {
```

```
 Outlier("IA", 1);
};
R_Date("AA82790 Ar/Ab.AB3.19.C14.02 charcoal 2",3037,50)
{
 Outlier("IA", 1);
};
R_Date("AA82794 Ar/Ab.AB3.22.C14.01 charcoal 2",2946,35)
{
 Outlier("IA", 1);
};
R_Date("AA82795 Ar/Ab.AB4.03.C14.04 charcoal 2",3060,40)
{
 Outlier("IA", 1);
};
R_Date("AA86868 Ar/Ab.AB4.06.C14.01 charcoal 2",2958,46)
{
 Outlier("IA", 1);
};
R_Date("AA82789 Ar/Ab.AB4.08.C14.01 charcoal 2",2949,51)
{
 Outlier("IA", 1);
};
R_Date("AA105117 Ar/Ab.AB4.46.C14.04 charcoal 2",2949,34)
{
 Outlier("IA", 1);
};
R_Date("AA105118 Ar/Ab.AB4.51.C14.03 charcoal 2",2958,35)
{
 Outlier("IA", 1);
};
R_Date("AA105120 Ar/Ab.AB4.59.C14.02 charcoal 2",3050,38)
```

```
 {
  Outlier("IA", 1);
 };
 Date ("Date Estimate Ar/Ab LB1-2 TPQ or Date")
 {
  color="Green";
 };
};
Boundary ("Ar/Ab TPQ to Date End")
{
 color="Red";
};
};
Sequence ()
{
Boundary ("Start Ar/Hn Late Bronze 1-2 TPQ = Stratum 2a-b")
{
 color="Red";
};
Phase ("Ar/Hn")
{
 R_Date("AA40143 Ar/Hn.F1.1B.C14.1 charcoal 2",2967,50)
 {
  Outlier("IA", 1);
 };
 R_Date("AA40144 Ar/Hn.TA1.A.C14.1 charcoal 2",3125,42)
 {
  Outlier("IA", 1);
 };
 R_Date("AA40145 Ar/Hn.F1.21.C14.1 charcoal 2",3050,42)
 {
```

```
   Outlier("IA", 1);
  };
  Date ("Date Estimate Ar/Hn LB1-2 TPQ or Date")
  {
   color="Green";
  };
 };
 Boundary ("Ar/Hn TPQ to Date End")
 {
  color="Red";
 };
};
};
Boundary ("Transition end LB2 to start Iron 1a")
{
 color="Red";
};
Phase ("Iron 1a overall")
{
 Sequence ("Iron 1a = 2c sequence Ar/Ge")
 {
  Boundary ("Start Iron 1a = Stratum 2c")
  {
   color="Red";
  };
  Phase ("Ar/Ge Stratum 2c")
  {
   R_Date("AA56971 Ar/Ge.T2E.210.C14.2 charcoal 2b or c",2925,35)
   {
    Outlier("IA", 1);
   };
```

```
R_Date("AA56972 Ar/Ge.T2E.218.C14.1 charcoal 2b or c",2903,34)
{
 Outlier("IA", 1);
};
R_Date("AA56974 Ar/Ge.T2D/e.11.C14.1 charcoal 2",2848,37)
{
 Outlier("IA", 1);
};
R_Date("AA66887 Ar/Ge.T15.B6.C14.2 2c?",2921,37)
{
 Outlier("IA", 1);
};
//AA66887 materials broadly LB to Iron 1
R_Date("AA66897 Ar/Ge.T2.E524.C14.1 charcoal 2b or c",2946,41)
{
 Outlier("IA", 1);
};
R_Date("AA40148 Ar/Ge.T01.03.C14.01 charcoal 2c",2768,40)
{
 Outlier("IA", 1);
};
R_Date("AA72055 Ar/Ge.T20.19.C14.1 charcoal 2c",2908,37)
{
 Outlier("IA", 1);
};
R_Date("AA72057 Ar/Ge.T20.25.C14.2 charcoal 2c",2925,37)
{
 Outlier("IA", 1);
};
R_Date("AA72058 Ar/Ge.T20.30.C14.1 charcoal 2c",2897,36)
{
```

```
 Outlier("IA", 1);
 };
 R_Date("AA92626 Ar/Ge.T21.02.C14.02 charcoal 2c",2909,42)
 {
 Outlier("IA", 1);
 };
 R_Date("AA66891 Ar/Ge.T15.C12.C14.1",2897,40)
 {
 Outlier("IA", 1);
 };
 //moved to 2c
 R_Date("AA105123 Ar/Ge.BC16.07.C14.01 charcoal 2 moved 2c burial",2895,39)
 {
 Outlier("IA", 1);
 };
 R_Date("AA105127 AR/Ge.K2.27.C14.01 tooth 2 moved to 2c",2884,39)
 {
 Outlier ("General",0.05);
 };
 Date ("Date Estimate Iron 1a - Ar/Ge")
 {
 color="Green";
 };
 Interval ("Duration Iron 1a - Ar/Ge");
};
Boundary ("End Iron 1a - Ar/Ge")
{
 color="Red";
};
};
Sequence ("Iron 1a - Ar/Ts")
```

```
{
 Boundary ("Start Iron 1a - Ar/Ts")
 {
  color="Red";
 };
 Phase ("Iron 1a or likely Iron 1a = 2c, some re-assigned from '2' - Ar/Ts")
 {
  R_Date("AA56977 Ar/Ts.C6.13.C14.1 charcoal 2c",2921,35)
  {
   Outlier("IA", 1);
  };
  R_Date("AA56984 Ar/Ts.SLT1.65 charcoal 2",2861,36)
  {
   Outlier("IA", 1);
  };
  R_Date("AA66876 Ar/Ts.SLT5.7.C14.2 charcoal 2",2869,39)
  {
   Outlier("IA", 1);
  };
  R_Date("AA95620 Ar/Ts.SLT13.15.C14.1 charcoal 2",2885,39)
  {
   Outlier("IA", 1);
  };
  Date ("Date Estimate Iron 1a - Ar/Ts")
  {
   color="Green";
  };
  Interval ("Duration Iron 1a - Ar/Ts");
 };
 Boundary ("End Iron 1a - Ar/Ts")
 {
```

```
   color="Red";
  };
 };
};
Boundary ("Transition Iron 1a to Iron 1b")
{
 color="Red";
};
Phase ("Iron 1b overall")
{
 Sequence ("Apparent Iron 1b presence = Stratum 2d at Ar/Ts")
 {
  Boundary ("Start Iron 1b Ar/Ts")
  {
   color="Red";
  };
  Phase ("Iron 1b Ar/Ts")
  {
   R_Date("AA66874 Ar/Ts.SLT5.4.C14.2 charcoal 2 reassigned",2668,39)
   {
    Outlier("IA", 1);
   };
   R_Date("AA92632 Ar/Ts.SLT10.14.C14.2 charcoal 2 reassigned",2702,38)
   {
    Outlier("IA", 1);
   };
   R_Date ("AA92629 Ar/Ts.SLT9.13.C14.1B charcoal 2 reassigned",2651,40)
   {
    Outlier("IA", 1);
   };
   R_Date ("AA92628 Ar/Ts.SLT9.12b.C14.1 charred pea 2 reassigned",2647,60)
```

```
 {
  Outlier ("General",0.05);
 };
 Date ("Date Estimate Ar/Ts Iron 1b")
 {
  color="Green";
 };
 Interval ("Duration Ar/Ts Iron 1b");
};
Boundary ("End Iron 1b Ar/Ts")
{
 color="Red";
};
};
Sequence ("Apparent Iron 1b presence = Stratum 2d at Ar/Ab")
{
Boundary ("Start Iron 1b Ar/Ab")
{
 color="Red";
};
Phase ("Iron 1b Ar/Ab")
{
 R_Date("AA105115 Ar/Ab.AB4.17.C14.03 charcoal 2 moved to 2d",2776,31)
 {
  Outlier("IA", 1);
 };
 R_Date("AA82788 Ar/Ab.AB4.06.C14.07 charcoal 2 moved to 2d",2774, 66)
 {
  Outlier("IA", 1);
 };
 R_Date("AA86869 Ar/Ab.AB4.06.C14.04 charcoal 2 moved to 2d",2877,46)
```

```
  {
   Outlier("IA", 1);
  };
  Date ("Date Estimate Ar/Ab Iron 1b")
  {
   color="Green";
  };
  Interval ("Duration Ar/Ab Iron 1b");
 };
 Boundary ("End Iron 1b Ar/Ab")
 {
  color="Red";
 };
};
};
Interval ("End Iron 1 to Iron 3");
Boundary ("Period Iron 1 to Iron 3")
{
 color="Red";
};
Sequence ("I3a sequence")
{
 Boundary ("Start I3a")
 {
  color="Red";
 };
 After ("Post 640 BC tpq for I3a")
 {
  C_Date ("TPQ 640BC", -640);
 };
 Phase ("I3a charcoal")
```

```
{
 Date ("=Minimum Felling Date TSA-14");
 //R_Date("AA40152 Gegharot T2.4 bone", 2324,42)
 //{
 //  Outlier ("General",0.05);
 // };
 //Materials LB to Iron 1 but date Iron 3 - mixed/contaminated? EXCLUDE
 R_Date("AA52904 Ar/Ts.C3.A7.C14.1 charcoal",2499,38)
 {
  Outlier("IA", 1);
 };
 //AA52904 is likely intrusive post into LB layer from Stratum 3
 //R_Date("AA56975 Ar/Ge.T2D/b.4.C14.1 charcoal", 2397,40)
 //{
 // Outlier("IA", 1);
 //};
 //insufficient contextual info for stratum determination - CUT
 R_Date("AA56988 Ar/Ts.SLT1.22.C14.1 charcoal", 2453,34)
 {
  Outlier("IA", 1);
 };
 R_Date("AA95621 Ar/Ts.SLT13.19.C14.2 charcoal", 2495,39)
 {
  Outlier("IA", 1);
 };
 R_Date("AA72371 Ar/Ts.WSH.40.C14.01 charcoal", 2542,42)
 {
  Outlier("IA", 1);
 };
 R_Date("AA96525 Ar/Ts.WSN.55.C14.01 charcoal", 2531,37)
 {
```

```
  Outlier("IA", 1);
 };
 R_Date("AA96526 Ar/Ts.WSN.93.C14.02 charcoal", 2513,42)
 {
  Outlier("IA", 1);
 };
 R_Date("AA96527 Ar/Ts.WSN.64.C14.01 charcoal", 2552,37)
 {
  Outlier("IA", 1);
 };
 R_Date("AA96521 Ar/Ts.WSAC2.24.C14.02 charcoal", 2554,37)
 {
  Outlier("IA", 1);
 };
 Date ("Date Estimate I3a")
 {
  color="Green";
 };
 Interval("Duration I3a");
};
Boundary ("End I3a")
{
 color="Red";
};
};
Sequence ("I3b")
{
 Boundary ("Start earlier I3b")
 {
  color="Red";
 };
```

```
After ("I3b = post-540BC as above flagstone floor")
{
 C_Date ("I3b", -540);
};
Phase ("I3b charcoal = earlier I3b TPQ")
{
 R_Date("AA66875 Ar/Ts.SLT6.5.C14.1 charcoal", 2483,42)
 {
  Outlier("IA", 1);
 };
 R_Date("AA72369 Ar/Ts.WSH.30.C14.02 charcoal", 2442,34)
 {
  Outlier("IA", 1);
 };
 R_Date("AA66880 Ar/Ts.WSC2.10.C14.1 charcoal",2494, 40)
 {
  Outlier("IA", 1);
 };
 R_Date("AA66882 Ar/Ts.WSE.3.C14.3 charcoal",2491, 56)
 {
  Outlier("IA", 1);
 };
 R_Date("AA72372 Ar/Ts.WSI.20.C14.01 charcoal", 2522,34)
 {
  Outlier("IA", 1);
 };
 R_Date("AA92841 Ar/Ts.WSI2.22.C14.04 charcoal", 2518,36)
 {
  Outlier("IA", 1);
 };
 R_Date("AA92842 Ar/Ts.WSAC.29.C14.02 charcoal", 2522,36)
```

```
{
 Outlier("IA", 1);
};
R_Date("AA96522 Ar/Ts.WSAC2.23.C14.03 charcoal", 2531,37)
{
 Outlier("IA", 1);
};
R_Date("AA96523 Ar/Ts.WSAC3.21.C14.01 charcoal", 2547,59)
{
 Outlier("IA", 1);
};
R_Date("AA72368 Ar/Ts.WSH.18.C14.01 charcoal", 2517,34)
{
 Outlier("IA", 1);
};
R_Date("AA72370 Ar/Ts.WSH.18.C14.03 charcoal", 2455,34)
{
 Outlier("IA", 1);
};
R_Date("AA92845 Ar/Ts.WSN.07.C14.02 charcoal", 2488,36)
{
 Outlier("IA", 1);
};
R_Date("AA101119 Ar/Ts.WSN.31.C14.01 charcoal", 2513,35)
{
 Outlier("IA", 1);
};
Date ("Date Estimate earlier I3b")
{
 color="Green";
};
```

```
 Interval ("Duration I3b");
 };
 Boundary ("End earlier I3b dates")
 {
  color="Red";
 };
};
Boundary ("From end earlier I3b to later I3b = Xerxes")
{
 color="Red";
};
Phase ("later I3b")
{
 Sequence ("later I3b")
 {
  Boundary ("Start later I3b Ar/Ts linked to Xerxes")
  {
   color="Red";
  };
  After ("486BC accession of Xerxes based on plates")
  {
   C_Date ("later I3b", -486);
  };
  Phase ("later I3b charcoal = after Xerxes accession context")
  {
   R_Date("AA72366 Ar/Ts.WSG.12.C14.04 charcoal", 2460,34)
   {
    Outlier("IA", 1);
   };
   R_Date("AA72367 Ar/Ts.WSG.12.C14.05 charcoal", 2438,34)
   {
```

```
   Outlier("IA", 1);
  };
  Date ("Date Estimate later I3b Ar/Ts")
  {
   color="Green";
  };
  Interval ("Duration later I3b Ar/Ts");
 };
 Boundary ("End later I3b Ar/Ts")
 {
  color="Red";
 };
};
R_Date("AA95619 Ar/Ts.SLT13.13.C14.1 charcoal", 2353,39)
{
 Outlier("IA", 1);
};
//reassigned to later I3b
Date ("Date Estimate later I3b overall")
{
 color="Green";
};
Interval ("Duration later I3b overall");
};
Boundary ("Transition end Iron 3b to Iron 4")
{
color="Red";
};
Sequence ()
{
 Boundary("Start of Iron 4")
```

```
{
 color="Red";
};
Phase ("Iron 4 based on 14C - sample intrusive to Stratum 2")
{
 R_Date("AA66889 Ar/Ge.T15.C21.C14.1 charcoal",1935,39)
 {
  Outlier("IA", 1);
 };
};
Boundary("End of Iron 4")
{
 color="Red";
};
};
Sequence ()
{
 Boundary("Start of Medieval")
 {
  color="Red";
 };
 Phase ("Medieval")
 {
  R_Date("AA52907 Ar/Ts.C5.17.C14.1 charcoal",1116,34)
  {
   Outlier("IA", 1);
  };
 };
 Boundary( "End of Medieval")
 {
  color="Red";
```

```
 };
};
Boundary ("Start Recent Wood")
{
 color="Red";
};
Phase ("19th Century AD")
{
 D_Sequence ("GEG-25A")
 {
  R_Date ("AA101106 1001-1010", 189, 26)
  {
   Outlier("RScaled",0.05);
  };
  Gap (11);
  R_Date ("AA101107 1012-1021", 78, 37)
  {
   Outlier("RScaled",0.05);
  };
  Gap(11);
  R_Date ("AA101108 1023-1032", 47, 34)
  {
   Outlier("RScaled",0.05);
  };
  Gap (11);
  R_Date ("AA101109 1034-1043", 147, 34)
  {
   Outlier("RScaled",0.05);
  };
  Gap (5.5);
  Date ("Last Ring GEG-25");
```

```
  };
 };
 Boundary( "End Sequence", Date(U(1000,2000)))
 {
  color="Red";
 };
};
Phase ("Summary LBA Chronology")
{
 Date ("=Date Estimate Ar/Ge earlier LB1 TPQ or Date");
 Date ("=Date Estimate Ar/Ge later LB1 TPQ or Date");
 Phase ("likely start LB2 TPQs from structure timbers Ar/Ge")
 {
  Date ("=Last Extant Ring GEG24A TPQ");
  Date ("=Minimum GEG23A TPQ");
 };
 Date ("=Date Estimate Ar/Ge LB2 TPQ or Date");
 Date ("=Date Estimate Ar/Ge LB2 General TPQ to Date");
 Date ("=Ar/Ge LB2 Destruction SL Weighted Av.");
 Date ("=Ar/Ge LB2 Destruction Tau_Boundary");
 Date ("=Date Estimate Ar/Ts LB1-2 TPQ or Date");
 Date ("=Date Estimate Ar/Ab LB1-2 TPQ or Date");
 Date ("=Date Estimate Ar/Hn LB1-2 TPQ or Date");
 Span ("Overall Duration ArAGATS LB Phases, LB1-LB2");
};
Difference ("Interval Between Defined Ar/Ge later LB1 and LB2","Date Estimate Ar/Ge LB2
TPQ or Date","Date Estimate Ar/Ge later LB1 TPQ or Date");
Correlation("Stratum 1a v Aparan III","Date Estimate Stratum 1a","Date Estimate Aparan III");
Correlation("Stratum 1a v. Karnut","Date Estimate Stratum 1a","AA-109426 Karnut 2016
Tomb 2 tooth");
```

Correlation("Stratum 1a1 v Aparan III","Date TPQ to Date Estimate Phase 1a1","Date Estimate Aparan III");
Correlation("Stratum 1a1 v. Karnut","Date TPQ to Date Estimate Phase 1a1","AA-109426 Karnut 2016 Tomb 2 tooth");
};

Alternative Model Code Treating Ar/Ge Specific 2a and 2b contexts as a single Sequence, versus two separate Sequences as above. This code replaces the code in the area indicated above by the two // notes. Note: the text in yellow highlight is NOT part of the OxCal Runfile

….

```
Sequence ("Ar/Ge 2a to 2b")
   {
    Boundary("Ar/Ge later 2a dates start")
    {
     color="Red";
    };
    Phase ("Ar/Ge 2a")
    {
     R_Date("AA40149 Ar/Ge.T02.23.C14.01 charcoal 2a",3098,42)
     {
      Outlier("IA", 1);
     };
     R_Date("AA40151 Ar/Ge.T02.18.C14.01 charcoal 2a",3151,50)
     {
      Outlier("IA", 1);
     };
```

```
 R_Date("AA72048 Ar/Ge.T2.E645.C14.1 charcoal 2a",3017,41)
 {
  Outlier("IA", 1);
 };
 R_Date("AA72049 Ar/Ge.T2.E626.C14.2 charcoal 2a",3117,41)
 {
  Outlier("IA", 1);
 };
 R_Date("AA95613 Ar/Ge.T31.41.C14.01 charcoal 2a?",3094,39)
 {
  Outlier("IA", 1);
 };
 R_Date("AA105124 Ar/Ge.K3.28.C14.03 charcoal 2a",3069,39)
 {
  Outlier("IA", 1);
 };
 R_Date("AA105137 Ar/Ge.K3.28.C14.01 charcoal 2a",3223,67)
 {
  Outlier("IA", 1);
 };
 R_Date("AA105138 Ar/Ge.K3.28.C14.02 charcoal 2a",3098,47)
 {
  Outlier("IA", 1);
 };
 Date ("Date Estimate Ar/Ge later LB1 TPQ or Date")
 {
  color="Green";
 };
 Interval ("Duration Ar/Ge later LB1");
};
Boundary ("Transition Ar/Ge 2a charcoal to Ar/Ge 2b")
```

```
{
 color="Red";
};
Phase ("Ar/Ge 2b")
{
 R_Date("AA52901 Ar/Ge.T02c.19.C14.1 charcoal 2b",2961,37)
 {
  Outlier("IA", 1);
 };
 //AA52901 - hard to push to Iron 1 based on stratigraphy so leave as LBA
 R_Date("AA56970 Ar/Ge.T2E.208.C14.3 charcoal 2b",3020,35)
 {
  Outlier("IA", 1);
 };
 R_Date("AA66886 Ar/Ge.T15.B3.C14.1 charcoal 2b",3081,37)
 {
  Outlier("IA", 1);
 };
 //R_Date("AA66888 Ar/Ge.T15.C14.C14.1 charcoal 2b",4313,39)
 //{
 // Outlier("IA", 1);
 //};
 //Outlier INITIAL CUT AS RESIDUAL
 R_Date("AA66890 Ar/Ge.T15.C25.C14.1 charcoal2b",2988,37)
 {
  Outlier("IA", 1);
 };
 R_Date("AA66896 Ar/Ge.T2.E522.C14.1 charcoal 2b",3082,35)
 {
  Outlier("IA", 1);
 };
```

```
R_Date("AA66898 Ar/Ge.T2.E513.C14.1 charcoal 2b",3001,40)
{
 Outlier("IA", 1);
};
R_Date("AA92625 Ar/Ge.T21.06.C14.02 charcoal 2b",2971,39)
{
 Outlier("IA", 1);
};
R_Date("AA95614 Ar/Ge.T31.07.C14.01 charcoal 2b?",3039,40)
{
 Outlier("IA", 1);
};
Label ("T27 - 2b?");
R_Date ("MAMS12406 C-AR-GEG T27 12A poplar",3033,25)
{
 Outlier("IA", 1);
};
R_Date ("MAMS12407A C-AR-GEG T27 5A wood charcoal",2990,31)
{
 Outlier("IA", 1);
};
R_Date ("MAMS12407B C-AR-GEG T27 5A",3032,26)
{
 Outlier("IA", 1);
};
R_Date("AA102811 Ar/Ge.T30.50.C14.01 charcoal 2b?",3049,41)
{
 Outlier("IA", 1);
};
R_Date("AA106847 Ar/Ge.T30.108.C14.01 charcoal 2 = 2b?",3019,27)
{
```

```
 Outlier("IA", 1);
};
R_Date ("MAMS12403 C-AR-GEG T27.11 A barley A", 2996,21)
{
 Outlier ("General",0.05);
};
R_Date ("MAMS12404 C-AR-GEG T27.11 B barley B", 2985,21)
{
 Outlier ("General",0.05);
};
R_Date ("AA104305A C-AR-GEG T27.11 C barley C", 2964,19)
{
 Outlier ("General",0.05);
};
R_Date ("AA104305B C-AR-GEG T27.11 C barley D", 2969,19)
{
 Outlier ("General",0.05);
};
//R_Date ("AA104305C C-AR-GEG T27.11 C barley E", 3051,21)
//{
// Outlier ("General",0.05);
//};
R_Date ("AA104305D C-AR-GEG T27.11 C barley F", 2980,21)
{
 Outlier ("General",0.05);
};
Date ("Date Estimate Ar/Ge LB2 TPQ or Date")
{
 color="Green";
};
Interval ("Duration Ar/Ge LB2");
```

```
    };
    Boundary ("End Ar/Ge 2b Phase",Date(U(-1251,-1093)))
    {
     color="Red";
    };
    //95.4% range for End Tau Boundary Phase 5 SL 2b dates minus AA104305C
   };
…..
```

	Model 2: no Outlier Models Amodel 68.5, Aoverall 83.1				**Model 3: with preferred combination of Outlier Models Applied (see Table S1) Amodel 90.5#, Aoverall 75.9**			
Element/Episode	**68.2% hpd Dates BC (whole range)**		**95.4% hpd Dates BC (whole range)**		**68.2% hpd Dates BC (whole range)**		**95.4% hpd Dates BC (whole range)**	
Date TPQ to Date Estimate Phase 1a1	3231	3065	3355	3018	3193	3067	3278	3007
Boundary Interval Between 1a1 and 1a?	3107	3001	3222	2960	3087	2977	3154	2930
Date Estimate Stratum 1a	3016	2969	3258	2914	2997	2913	3007	2906
Duration Stratum 1a	*0*	*36*	*0*	*88*	*0*	*41*	*0*	*89*
Date TPQ to date Estimate Time Period Between 1a and 1b	2960	2888	2987	2852	2914	2873	2948	2852
Date Estimate Stratum 1b Charcoal	2846	2761	2896	2732	2844	2795	2867	2757
Date Estimate Stratum 1b Terminal	2803	2707	2873	2682	2814	2764	2819	2707
Date Estimate Stratum 1b Overall	2838	2740	2896	2701	2841	2778	2864	2723
Boundary End 1b	2795	2687	2869	2665	2806	2748	2810	2683
Boundary Duration of time between EB and the MB presence	2538	2004	2684	1828	2571	2065	2700	1853
Boundary Start MBA Presence	1881	1702	2023	1639	1886	1704	2035	1642
Duration MBA Presence	*0*	*136*	*0*	*329*	0	141	0	346

Boundary End MBA Intrusive Presence	1776	1626	1857	1582	1772	1624	1858	1576
Boundary Period of Time MBA Presence to LBA Occupation	1621	1521	1754	1514	1619	1523	1746	1514
Minimum Felling Date GEG-26	1540	1501	1546	1491	1540	1504	1546	1491
Boundary Start Early LB1	1511	1461	1528	1432	1514	1466	1530	1441
Date Estimate Ar/Ge Earlier LB1 TPQ or Date	1500	1449	1521	1427	1506	1457	1524	1435
Boundary Transition earlier LB1 to Later LB1	1469	1420	1503	1409	1481 1486*	1430 1431*	1507 1511*	1415 1416*
Date Estimate Ar/Ge Later LB1 TPQ or Date	1409	1300	1439	1248	1382 1346*	1296 1253*	1422 1408*	1246 1227*
Duration Ar/Ge Later LB1	*0*	*123*	*0*	*219*	*0* *64**	*110* *188**	*0* *8**	*223* *218**
Date Estimate Ar/Ge LB2 (Phase 2b) TPQ or Date	1237	1201	1274	1176	1234 1244*	1205 1204*	1264 1274*	1186 1182*
Duration Ar/Ge LB2	*0*	*59*	*0*	*130*	*0* *0**	*45* *64**	*0* *0**	*106* *121**
Boundary End Ar/Ge 2b Phase	1248	1185	1253	1156	1221 1220*	1194 1188*	1232 1251*	1156 1153*
Date Estimate Ar/Ge Phase 2 General material TPQ to Date	1265	1195	1307	1164	1239	1184	1278	1146

Boundary End Ar/Ge 2b general material	1230	1159	1253	1135	1211	1158	1223	1113
Date Estimate Ar/Ts LB1-2 TPQ to Date	1366	1287	1411	1241	1379	1205	1432	1158
Boundary End Ar/TS LB1-2	1312	1239	1345	1187	1194	1140	1217	1107
Date Estimate Ar/Ab LB1-2 TPQ or Date	1291	1201	1347	1162	1252	1171	1317	1121
Boundary Ar/Ab TPQ to Date End (2b)	1248	1166	1290	1124	1205	1126	1129	1083
Date Estimate Ar/Hn LB1-2 TPQ or Date	1364	1230	1417	1171	1352	1217	1410	1149
Boundary Ar/Hn TPQ to Date End (2b)	1300	1166	1366	1120	1276	1136	1348	1088
Boundary Transition End LB2 to Start Iron 1a (i.e. LB3 abandonment/hiatus)	1183	1113	1201	1073	1137	1062	1169	1037
Date Estimate Iron 1a Ar/Ge	1111	1050	1141	1015	1072	1024	1097	1002
Duration Iron 1a Ar/Ge	*0*	*49*	*0*	*119*	*0*	*42*	*0*	*106*
Date Estimate Iron 1a Ar/Ts	1123	1044	1164	1003	1074	1018	1103	988
Duration Iron 1a Ar/Ts	*0*	*54*	*0*	*134*	*0*	*44*	*0*	*111*
Boundary Transition Iron 1a to Iron 1b	1081	978	1116	821	1044	967	1072	912

Date Estimate Ar/Ts Iron 1b	893	788	952	717	841	785	898	743
Duration Ar/Ts Iron 1b	*0*	*148*	*0*	*276*	*0*	*78*	*0*	*200*
Date Estimate Ar/Ab Iron 1b	975	821	1058	766	963	861	1006	777
Duration Ar/Ab Iron 1b	*0*	*138*	*0*	*293*	*0*	*124*	*0*	*280*
Boundary Period Iron 1 to Iron 3 (i.e. missing Iron 2 hiatus)	685	544	825	535	676	543	783	539
Interval [between] End Iron 1 to Iron 3	*0*	*164*	*0*	*259*	*0*	*206*	*0*	*238*
Date Estimate Iron 3a (I3a)	588	535	631	534	602	543	618	538
Duration I3a	*0*	*44*	*0*	*87*	*0*	*36*	*0*	*76*
Date Estimate Earlier I3b	539	521	545	504	542	527	545	516
Duration Earlier I3b	*0*	*19*	*0*	*46*	*0*	*12*	*0*	*30*
Date Estimate Later I3b Ar/Ts	485	412	491	336	482	417	491	367
Duration Later I3b Ar/Ts	*0*	*54*	*0*	*163*	*0*	*55*	*0*	*148*
Date Estimate Later I3b Overall	502	381	525	238	499	385	531	248
Duration Later I3b Overall	*0*	*202*	*0*	*395*	*19*	*209*	*0*	*409*
Boundary Transition End Iron 3b to Iron 4	467	294	477	91	459	298	484	96

Table S2. Selected calendar age ranges from the ArAGATS Bayesian Chronological Models, Model 1 (no outlier models applied) and Model 3 (the preferred model applying the OxCal RScaled Outlier model to the wiggle-match samples, the General Outlier model to the short/shorter-lived samples, and the Charcoal Plus Outlier model to the dates on charcoal samples: see Table S1). Model 3 results

are shown in detail in Figures 2, 5 and 9, and Figure S1. *Values are from the alternative model (Model 3a), see Table S1, where the contiguous Stratum 2a > Stratum 2b Gegharot sequence is employed – see also Figure S1K. #Amodel values over various runs ranged from ca. 80 to 91.

Table S3. The data listing for a file "/IA.prior" for use with OxCal in order to run the Charcoal Plus Outlier model in an OxCal runfile with the line of code "Outlier_Model("IA",Prior("Charcoal_Plus"),U(0,3),"t");" (compare with the rounded data for the same file in Table S6 in DEE et al. 2013 electronic supplementary material at: 2013http://rspa.royalsocietypublishing.org/content/royprsa/suppl/2013/09/02/rspa.2013.0395.DC1/rspa20130395supp1.pdf). We thank Michael Dee for his assistance.

-10	4.31299E-05
-9.9	4.76659E-05
-9.8	5.2679E-05
-9.7	5.82193E-05
-9.6	6.43423E-05
-9.5	7.11092E-05
-9.4	7.85879E-05
-9.3	8.6853E-05
-9.2	9.59874E-05
-9.1	0.000106083
-9	0.000117239
-8.9	0.000129569
-8.8	0.000143196
-8.7	0.000158257
-8.6	0.000174901
-8.5	0.000193295
-8.4	0.000213624

-8.3	0.000236091
-8.2	0.000260921
-8.1	0.000288362
-8	0.000318689
-7.9	0.000352206
-7.8	0.000389248
-7.7	0.000430186
-7.6	0.000475429
-7.5	0.00052543
-7.4	0.00058069
-7.3	0.000641762
-7.2	0.000709257
-7.1	0.00078385
-7	0.000866288
-6.9	0.000957396
-6.8	0.001058086
-6.7	0.001169366
-6.6	0.00129235
-6.5	0.001428267
-6.4	0.001578479
-6.3	0.00174449
-6.2	0.001927959

-6.1	0.002130724
-6	0.002354815
-5.9	0.002602473
-5.8	0.002876177
-5.7	0.003178667
-5.6	0.003512971
-5.5	0.003882433
-5.4	0.004290752
-5.3	0.004742014
-5.2	0.005240736
-5.1	0.005791909
-5	0.00640105
-4.9	0.007074254
-4.8	0.00781826
-4.7	0.008640513
-4.6	0.009549244
-4.5	0.010553547
-4.4	0.011663473
-4.3	0.012890131
-4.2	0.014245798
-4.1	0.015744042
-4	0.017399857

-3.9	0.019229816
-3.8	0.021252233
-3.7	0.02348735
-3.6	0.025957536
-3.5	0.028687514
-3.4	0.031704606
-3.3	0.035039009
-3.2	0.038724094
-3.1	0.042796742
-3	0.047297715
-2.9	0.052272059
-2.8	0.057769559
-2.7	0.063845237
-2.6	0.070559899
-2.5	0.077980749
-2.4	0.086182056
-2.3	0.095245902
-2.2	0.105263
-2.1	0.116333607
-2	0.128568519
-1.9	0.142090188
-1.8	0.157033944

-1.7	0.173549348
-1.6	0.191801692
-1.5	0.211973652
-1.4	0.234267116
-1.3	0.258905203
-1.2	0.286134501
-1.1	0.31622753
-1	0.349485469
-0.9	0.386241177
-0.8	0.426862516
-0.7	0.471756039
-0.6	0.521371054
-0.5	0.576204127
-0.4	0.636804044
-0.3	0.70377731
-0.2	0.777794215
-0.1	0.859595547
0	0.95
0.1	0.045241871
0.2	0.040936538
0.3	0.037040911
0.4	0.033516002

0.5	0.030326533
0.6	0.027440582
0.7	0.024829265
0.8	0.022466448
0.9	0.020328483
1	0.018393972
1.1	0.016643554
1.2	0.015059711
1.3	0.01362659
1.4	0.012329848
1.5	0.011156508
1.6	0.010094826
1.7	0.009134176
1.8	0.008264944
1.9	0.007478431
2	0.006766764
2.1	0.006122821
2.2	0.005540158
2.3	0.005012942
2.4	0.004535898
2.5	0.00410425
2.6	0.003713679

2.7	0.003360276
2.8	0.003040503
2.9	0.002751161
3	0.002489353
3.1	0.00225246
3.2	0.00203811
3.3	0.001844158
3.4	0.001668663
3.5	0.001509869
3.6	0.001366186
3.7	0.001236176
3.8	0.001118539
3.9	0.001012096
4	0.000915782
4.1	0.000828634
4.2	0.000749779
4.3	0.000678428
4.4	0.000613867
4.5	0.00055545
4.6	0.000502592
4.7	0.000454764
4.8	0.000411487

4.9	0.000372329
5	0.000336897
5.1	0.000304837
5.2	0.000275828
5.3	0.00024958
5.4	0.000225829
5.5	0.000204339
5.6	0.000184893
5.7	0.000167298
5.8	0.000151378
5.9	0.000136972
6	0.000123938
6.1	0.000112143
6.2	0.000101472
6.3	9.18152E-05
6.4	8.30779E-05
6.5	7.5172E-05
6.6	6.80184E-05
6.7	6.15456E-05
6.8	5.56888E-05
6.9	5.03893E-05
7	4.55941E-05

7.1	4.12552E-05
7.2	3.73293E-05
7.3	3.37769E-05
7.4	3.05626E-05
7.5	2.76542E-05
7.6	2.50226E-05
7.7	2.26414E-05
7.8	2.04867E-05
7.9	1.85372E-05
8	1.67731E-05
8.1	1.5177E-05
8.2	1.37327E-05
8.3	1.24258E-05
8.4	1.12434E-05
8.5	1.01734E-05
8.6	9.20529E-06
8.7	8.32929E-06
8.8	7.53665E-06
8.9	6.81945E-06
9	6.17049E-06
9.1	5.58329E-06
9.2	5.05197E-06

9.3	4.57121E-06
9.4	4.1362E-06
9.5	3.74259E-06
9.6	3.38644E-06
9.7	3.06417E-06
9.8	2.77258E-06
9.9	2.50873E-06
10	2.27E-06